

Evaluation of the Tubulin-Bound Paclitaxel Conformation: Synthesis, Biology, and SAR Studies of C-4 to C-3' Bridged Paclitaxel Analogues

Thota Ganesh,[†] Chao Yang,[†] Andrew Norris,[†] Tom Glass,[†] Susan Bane,^{‡,*} Rudravajhala Ravindra,[‡] Abhijit Banerjee,[‡] Belhu Metaferia,[†] Shala L. Thomas,[‡] Paraskevi Giannakakou,[‡] Ana A. Alcaraz,[§] Ami S. Lakdawala,[§] James P. Snyder,^{§,*} and David G. I. Kingston^{†,*}

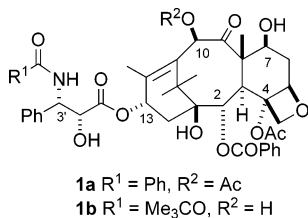
Department of Chemistry, M/C 0212, Virginia Polytechnic Institute and State University, Blacksburg, Virginia 24061, Department of Chemistry, State University of New York at Binghamton, Binghamton, New York 13902, Winship Cancer Institute, Emory University School of Medicine, Atlanta, Georgia 30322, and Department of Chemistry, Emory University, Atlanta, Georgia 30322

Received September 11, 2006

The important anticancer drug paclitaxel binds to the β -subunit of the $\alpha\beta$ -tubulin dimer in the microtubule in a stoichiometric ratio, promoting microtubule polymerization and stability. The conformation of microtubule-bound drug has been the subject of intense study, and various suggestions have been proposed. In previous work we presented experimental and theoretical evidence that paclitaxel adopts a T-shaped conformation when it is bound to tubulin. In this study we report additional experimental data and calculations that delineate the allowable parameters for effective paclitaxel–tubulin interactions.

Introduction

The natural product paclitaxel (PTX)^a (**1a**) and its closely related semisynthetic analogue docetaxel (DTX, **1b**) are clinically approved drugs for several tumor malignancies, including breast, lung, and ovarian carcinomas,¹ while PTX has recently been shown to be effective in reducing the risk of restenosis following percutaneous coronary intervention.² These molecules, in common with several other recently discovered natural products such as the epothilones,³ discodermolide,⁴ laulimalide,⁵ and eleutherobin,⁶ act by promoting the polymerization of tubulin to stabilized microtubules, leading to cell cycle arrest at the G₂/M phase and hence to apoptotic cell death.^{7–10} Although PTX has been shown to influence the phosphorylation and translocation of cell signaling factors,¹¹ its clinical activity is believed to be directly related to its microtubule-binding activity.¹⁰



PTX is a complex molecule and is expensive to produce from natural sources. Ideally, future generations of this class of drugs should have much simpler structures, while retaining the activity of the parent drug. Any rational design of improved or simplified analogues would be greatly enhanced by knowledge of the “pharmacophore” of PTX, which can be approximately equated with the conformation of this compound in its binding site on β -tubulin. Thus the elucidation of this pharmacophore is a matter of great practical as well as theoretical significance.

* To whom correspondence should be addressed. Phone: 540-231-6570. Fax: 540-231-3255. E-mail: dkingston@vt.edu.

[†] Virginia Polytechnic Institute and State University.

[‡] State University of New York at Binghamton.

[§] Department of Chemistry, Emory University.

^a Emory University School of Medicine.

^b Abbreviations: PTX, paclitaxel; NAMFIS, NMR analysis of molecular flexibility in solution.

The nature of the binding of PTX to tubulin polymer is not yet known in complete detail, although a significant advance was made by the determination of the electron crystallographic structure of $\alpha\beta$ -tubulin, initially at 6.5 Å and later improved to 3.7 Å.^{12,13} Although the latter work was carried out with PTX-stabilized zinc-induced sheets, it lacks the resolution to define the detailed conformation of paclitaxel on the tubulin polymer. PTX is a large and conformationally mobile molecule, with rotatable groups at C-2, C-4, C-10, and C-13 appended to an essentially rigid tetracyclic ring system. The question of the preferred binding conformation of PTX on the binding site of the tubulin receptor is thus a complicated one.

Previous studies of the bioactive conformation have used evidence from NMR and modeling analyses to suggest three different models for the bioactive conformation of PTX. A “nonpolar” conformation with clustering of the C-2 benzoate and the C-3' benzamido group of the side chain was proposed as the bioactive conformer on the basis of single conformation NMR studies in nonpolar solvents.^{14–16} Similar NMR studies in polar solvents revealed a hydrophobically collapsed conformation with clustering of the C-2 benzoate and the C-3' phenyl group. This led to the proposal that the “polar” conformation is the bioactive form.^{17–21} Although most of the reports assumed a single conformation, deconvolution for PTX in CDCl₃²² and D₂O/DMSO-*d*₆²³ makes it clear that the molecule adopts 8–14 conformations, no one of which achieves a population above 30%. A second approach has used spectroscopic studies of tubulin-bound PTX. One study using REDOR NMR provided F–¹³C distances of 9.8 and 10.3 Å between the fluorine of a 2-(*p*-fluorobenzoyl)PTX and the C-3' amide carbonyl and C-3' methine carbons, respectively.²⁴ A related solid-state study employing the NMR RFDR method reported a distance of 5.5 Å between the fluorines of 2-(*p*-fluorobenzoyl)-3'-(*p*-fluorophenyl)-10-acetyl-DTX.²¹ Both of the latter investigations singled out the polar conformation of PTX as the bound rotamer.

The “polar” and “nonpolar” conformations have inspired a number of elegant synthetic studies designed to generate constrained analogues which maintain these conformations. However, with one exception,²⁵ none of the constrained analogues synthesized to date based on these conformations have yielded analogues with both tubulin polymerization and cyto-

toxic activities equal to or greater than those of PTX itself. Thus, various compounds designed to mimic the polar conformation have been prepared, but these compounds were either inactive²⁶ or less active than PTX.²⁷ Similarly, constrained analogues based on the nonpolar conformation were also less active than PTX.^{28–31} Two recent studies have presented two bridged taxanes with microtubule stabilizing capacity equivalent to paclitaxel, but with diminished cytotoxicity.³² In a review of taxane-bridging strategies, we have detailed the need for a new approach and outlined our initial efforts in this direction.³³

Results and Discussion

Design and Development of T-Taxol Models. As outlined above, conception of various bridged analogues as candidates for binding at the taxane site on β -tubulin followed from hypotheses regarding the nature of the binding pose. In this respect, the T-Taxol conformation is no exception. The groundbreaking work of Nogales, Wolf, and Downing that solved the structure of $\alpha\beta$ -tubulin by electron crystallography (EC) was made possible, in part, by stabilizing sheets of polymerized tubulin with zinc cations and PTX.¹² The 3.7 Å resolution structure, however, was unable to reveal paclitaxel's conformation and binding pose. The molecule's location was nonetheless represented by the single-crystal X-ray structure of docetaxel introduced as a ligand place-holder.³⁴ To overcome the paucity of structural detail for the ligand, a strategy combining the low-resolution EC data and higher resolution small molecule structural data was employed.

Specifically, an analysis of the 2D NMR spectra of PTX in both CDCl₃²² and D₂O/DMSO-*d*₄²³ using NAMFIS methodology³⁵ indicated that the compound adopts over a dozen conformations, among which a T-Taxol or butterfly conformation contributes mole fractions of 0.04 (4% population) and 0.02 (2%), respectively, in the two solvents. EC-density fitting of both the NMR conformations and a number of taxane X-ray structures led to the postulate that the T-Taxol conformation is the bioactive form.³⁶ This model posits that the centroid of the C-2 benzoate phenyl of PTX is essentially equidistant from the centroids of the phenyl and benzamide-phenyl groups emanating from the C-3' position; thus, the T-shaped conformation. A singular advantage of this structural motif is that when the T-Taxol conformer is nestled into the electron crystallographic density of the PTX-tubulin complex, His227 of the protein is interposed between the C-3' benzamido and C-2 benzoyl phenyl rings of PTX. Hydrophobic collapse of the taxane phenyl groups in this sector of the binding pocket is thereby eliminated as a feature of ligand binding.³⁶

Examination of the T-shape shows that the C-3' phenyl and C-4 OAc moieties are juxtaposed, the distance between the *o*-phenyl and methyl centroid hydrogens being only 2.5 Å (Figure 1).³⁷ If the T-Taxol model accurately reflects the PTX-tubulin interaction, conformationally constrained analogues which maintain this juxtaposition should yield PTX analogues with improved tubulin-binding properties. The entropic penalty resulting from binding to tubulin is greatly reduced in the constrained analogues. As a result these analogues were expected to show a higher bioactivity than PTX itself, particularly when the bridge is short and emanates from the C-3' phenyl ortho center. The predictions were vindicated by our preliminary results in this area, which demonstrated that taxoid design and synthesis based on the T-Taxol conformation yields compounds with improved activity in both tubulin polymerization and cytotoxicity assays.^{37,38} Very recently we have presented additional experimental evidence from REDOR NMR and mo-

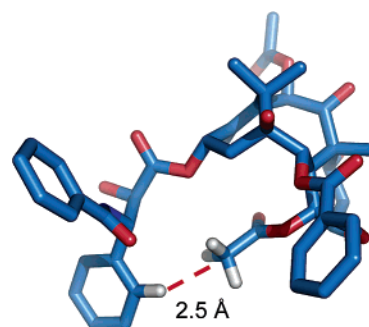


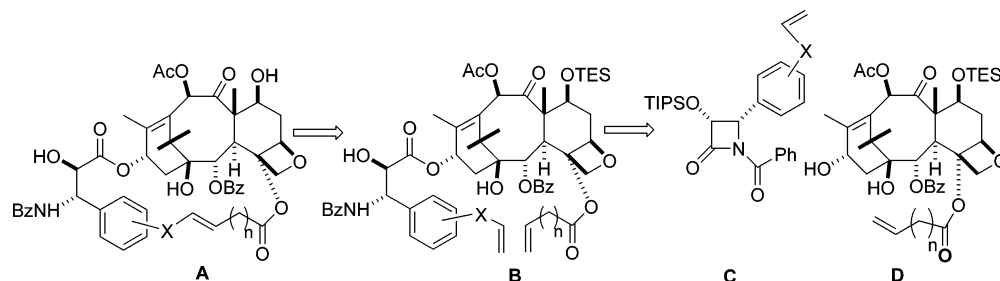
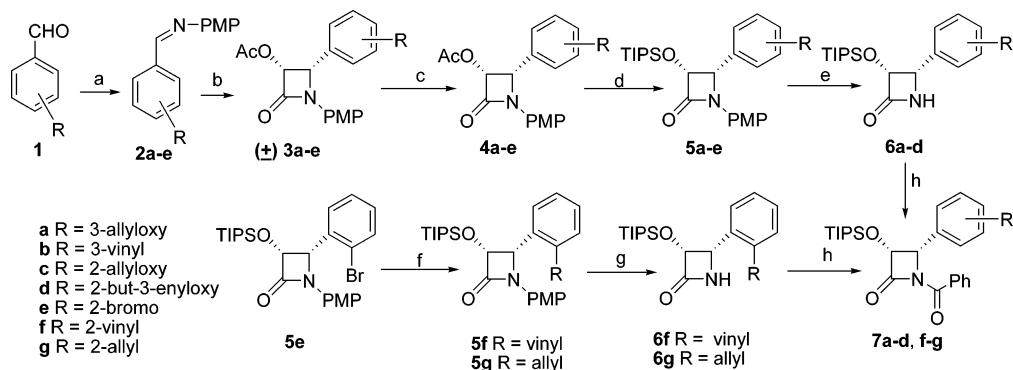
Figure 1. T-Taxol illustrating the short H–H distance between the centroid of the C-4 acetate methyl group and the ortho-position of the C-3' phenyl ring.

lecular modeling for the T-Taxol model,³⁹ and we have also shown that the model can guide the synthesis of cytotoxic analogues from non-cytotoxic precursors.⁴⁰ In this paper, we describe the synthesis, biological evaluation, and molecular modeling for an expanded set of highly active C-4 to C-3' constrained analogues.

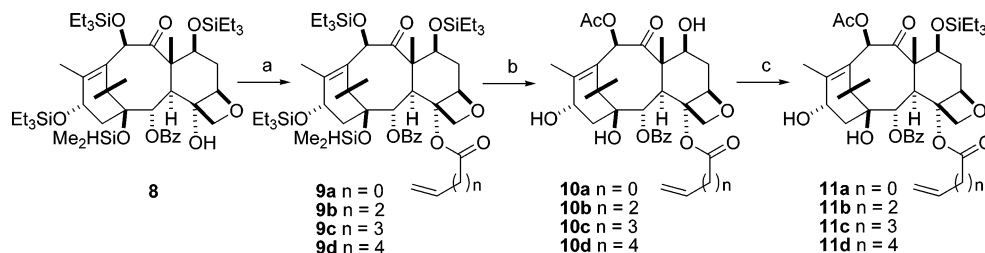
Synthesis of Macrocyclic PTX analogues. We selected the well-established ring-closing metathesis strategy⁴¹ for the crucial macrocyclization step (Scheme 1), as it has proved highly efficacious for generation of macrocyclic taxoids.²⁷ The proposed macrocyclic analogues (A) were envisioned to arise from the open chain ω,ω' -dienes B, which can be derived from modified β -lactam (C) and baccatin III (D) derivatives.

The retrosynthesis shown in Scheme 1 required the preparation of several β -lactam derivatives with a substituent at either the ortho or meta position of the phenyl group and various C-4 modified baccatin derivatives. The syntheses of the β -lactam derivatives were accomplished by application of literature procedures^{42,43} (Scheme 2). The syntheses of (\pm)- β -lactams (3a–e) were achieved starting from 3-allyloxy, 3-vinyl, 2-allyloxy, 2-butenyloxy, and 2-bromo benzaldehydes (1a–e) through the *N*-(*p*-methoxy phenyl) (PMP) protected imines 2a–e. Resolution of the (\pm)- β -lactams (3a–e) was carried out with lipase PS (Amano) to yield the desired enantiomeric acetates (+)-(4a–e), along with undesired enantiomeric (–)-alcohols (not shown) in more than 95% yield.^{43,44} Functional group manipulations on 4a–e generated the triisopropylsilyl ether intermediates 5a–e. The 4-(2-bromophenyl) derivative (5e) on Stille coupling⁴⁵ with vinyltributyltin and allyltributyltin produced the 4-(2-vinylphenyl) and 4-(2-allylphenyl) lactam intermediates 5f,g, respectively. The PMP-protected intermediates 5a–d and 5f,g were deprotected with ceric ammonium nitrate to produce secondary amides (6a–d,f,g), which were treated with benzoyl chloride in the presence of triethylamine and dimethylaminopyridine to result in the (+)-(3*R*,4*S*)-1-benzoyl-3-triisopropylsilyloxy-4-(aryl)-azetidin-2-ones 7a–d and 7f,g (Scheme 2)

Synthesis of the baccatin derivatives 11a–d started with the known 4-deacetylbaccatin derivative 8.⁴⁶ Initial attempts to acylate the hindered C-4 hydroxy group using the DCC/DMAP method resulted in unacceptable yields of C-4 acyl derivatives, but the use of acid chloride and LiHMDS in THF at 0 °C gave the C-4 acyl baccatin derivatives 9a–d with yields ranging from 50 to 78%. A minor product acylated at the C-4 position, but with a loss of the 1-dimethylsilyl group, was always obtained in this step, and it was used for the subsequent step. Global deprotection of 9a–d using HF/pyridine, followed by selective C-10 acetylation⁴⁷ with 0.1 mol % of CeCl₃ and acetic anhydride in tetrahydrofuran, gave greater than 90% yields of the desired 10-acetyl derivatives (10a–d). Selective protection of the C-7

Scheme 1. Retrosynthetic Logic for Preparation of Macrocyclic Taxanes **A** from ω,ω' -Dienes **B** Derived from β -Lactams **C** and Baccatins III **D****Scheme 2.** Synthesis of β -Lactams **7^a**

^a a. *p*-MeOC₆H₄NH₂, MgSO₄, CH₂Cl₂ (100%); b. CH₃COOCH₂COCl, Et₃N or Pr₂EtN, -78 °C to room temp, 12 h (80–85%); c. lipase PS (Amano), phosphate buffer, pH = 7.2, CH₃CN, 24 h to 12d (90–95%); d. i, 1 M, KOH, THF, 0 °C (quantitative); ii, TIPSOS, imidazole, DMF (90–94%); e. CAN, CH₃CN, 0 °C (65–92%); f. Pd₂(dba)₃, Ph₃P, dioxane, 80 °C, vinyltributyltin (**5f**, 80%), allyltributyltin (**5g**, 84%); g. (i) CAN, CH₃CN, -5 °C (65–70%), (ii) PhCOCl, Et₃N, DMAP, CH₂Cl₂ (**7f**, 86%, and **7g**, 90%); h. PhCOCl, Et₃N, DMAP, CH₂Cl₂ (85–95%).

Scheme 3. Synthesis of Baccatins III **11a–d^a**

^a a. LHMDS, THF, 0 °C, acryloyl chloride (**9a**, 52%), 4-pentenoyl chloride (**9b**, 78%), 5-hexenoyl chloride (**9c**, 71%), 6-heptenoyl chloride (**9d**, 50%); b. i, HF⁺Py, THF (*n* = 0, 60%, *n* = 2, 91%, *n* = 3, 80%, *n* = 4, 44%), ii, CeCl₃, Ac₂O, THF (**10a**, *n* = 0, 89%), (**10b**, *n* = 2, 92%), (**10c**, *n* = 3, 89%), (**10d**, *n* = 4, 95%); c. Triethylsilyl chloride, imidazole, DMF (**11a**, *n* = 0, 87%), (**11b**, *n* = 2, 85%), (**11c**, *n* = 3, 72%), (**11d**, *n* = 4, 83%).

hydroxyl as its triethylsilyl ether afforded the C-4 alkenoyl baccatins **11a–d** in good yields (Scheme 3).

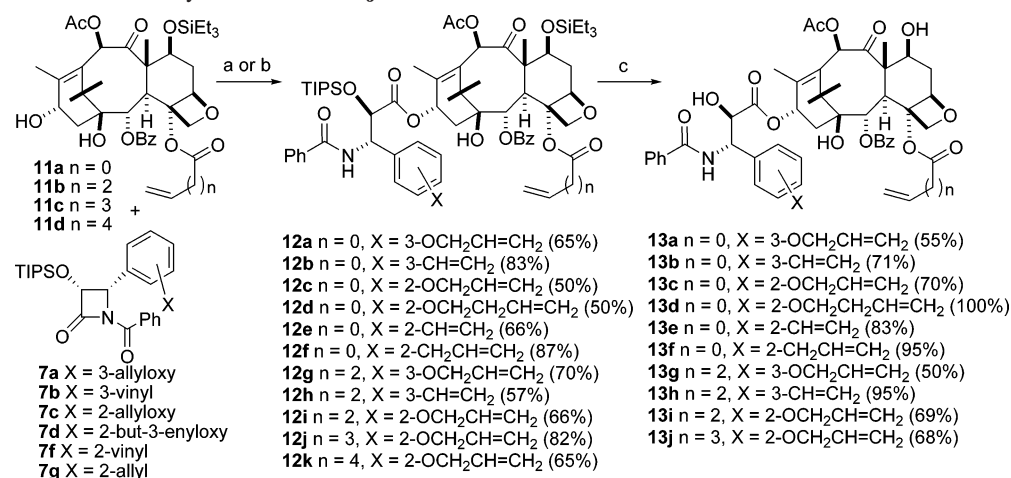
Having prepared the desired baccatin III derivatives (**11a–d**) and β -lactam derivatives (**7a–d, f, g**), we synthesized the ω,ω' -diene taxoid precursors **12a–k**, with yields ranging from 50 to 92% using the Holton–Ojima coupling protocols⁴⁸ (Scheme 4). These dienes set the stage for the crucial ring-closing metathesis reaction.

Our initial studies of the cyclization reaction employed the ω,ω' -diene substrates **12g** and **12h** and first generation Grubb's catalyst in dichloromethane under high dilution condition,³⁸ but in later studies the second generation Grubbs's catalyst under the same high dilution conditions proved to give superior results. In this particular transformation the open chain diene substrates **12f–h** produce exclusively the *Z* alkenes **14f–h**, while the dienes **12a** and **12c** gave exclusively the *E*-alkenes **14a** and **14c**. The remaining dienes **12d** and **12i–k** yielded *E/Z* mixtures **14d**, **14i–k** which were separable by silica gel chromatography. All the cyclic derivatives **14** were subjected to deprotection with HF⁺Py in tetrahydrofuran to produce the bridged paclitaxel analogues **15** in satisfactory yields. In most cases the more stable

E forms of the bridging double bond were obtained, but for reasons we do not fully understand, only the *Z* form of compound **15f** was obtained. The *Z* configuration was assigned on the basis of the coupling constant of 11.4 Hz for the olefinic protons of the bridging double bond. It is noteworthy that compound **23**, with a *m*-methoxybenzoyl group at C-2, gave a mixture of the *Z*-alkene **27** and the unconjugated *E*-alkene **24** on olefin metathesis (see below).

In a preliminary effort to explore the absence of *E*-**15f** from the reactions just described, we carried out density functional theory (DFT) single point calculations on MMFFs *E* and *Z* optimized structures (model: B3LYP/6-31G**). Indeed, in contrast to the experimental outcome, the *E*-form is predicted to be more stable than the *Z*-isomer. Preliminary DFT optimization of truncated forms of *Z*-**15f** and *E*-**15f** provided a similar relative energy. We speculate that the outcome of ring closure metathesis for **15f** is not governed by product thermodynamics, but by the geometry of the bulky Grubbs catalyst in complex with the starting diene or the corresponding transition state.

Finally the saturated bridged paclitaxels **16** were prepared by hydrogenation of **15** (Scheme 5). It is worth noting here that

Scheme 4. Synthesis of Bis-Alkenyl Baccatins **13a–j**^a

^a a. LHMDS, THF, $-40\text{ }^{\circ}\text{C}$; b. NaH, THF, $0\text{ }^{\circ}\text{C}$ to room temp; c. HF \cdot Py in THF, $0\text{ }^{\circ}\text{C}$ to room temp, 12 h.

neither the dienes **12b** and **12e** nor their 2',7-silyl deprotected derivatives **13b** and **13e** yielded any of the expected olefin metathesis products **14b** and **14e** under any of the several ring-closing metathesis conditions tested using either Grubbs catalysts, presumably due to the ring strain inherent in forming the short bridges required for these compounds.

Development of Bridged PTX Analogues with Improved Bioactivities. As pointed out in the introduction, a key test of the proposed bioactive conformations is the synthesis of a constrained analogue that mimics this conformation and possesses an equal or greater bioactivity with respect to the parent compound. In our approach to the synthesis of such a conformationally constrained analogue, we initially synthesized the 21- and 19-membered macrocyclic analogues **15g** and **15h** with eight and six atoms, respectively, in a bridge between the C-4 acetyl group and the meta-position of the C-3' phenyl group of PTX.³⁸ These analogues exhibited modest cytotoxicity against the A2780 ovarian cancer cell line and significant tubulin polymerization (TP) activity, but the activities were considerably less than those of PTX. The reduced activity of **15g** was explained by a combination of NMR-NAMFIS analysis, which deconvolutes NMR virtual structures to individual conformers in solution, and a computational analysis of taxane-tubulin complexes. These studies indicated that compound **15g**, although capable of adopting the bioactive T-form, is seated higher in the PTX-binding pocket as a result of close contact between the propene moiety of the tether and Phe270 of the protein.^{38,49}

In the present study, we initially synthesized the dihydro derivatives **16g** and **16h** by hydrogenation of **15g** and **15h**, respectively, to evaluate whether increased flexibility of alkane-bridged macrocyclic taxoids might alleviate the unfavorable interaction with Phe270.⁴⁹ However, the bioactivities of these compounds with saturated bridges were even less than those of the unsaturated compounds **15g** and **15h**. Surprisingly, the open chain analogues **13g** and **13h** showed better cytotoxicities than their macrocyclic counterparts **15g** and **15h** (Table 1).

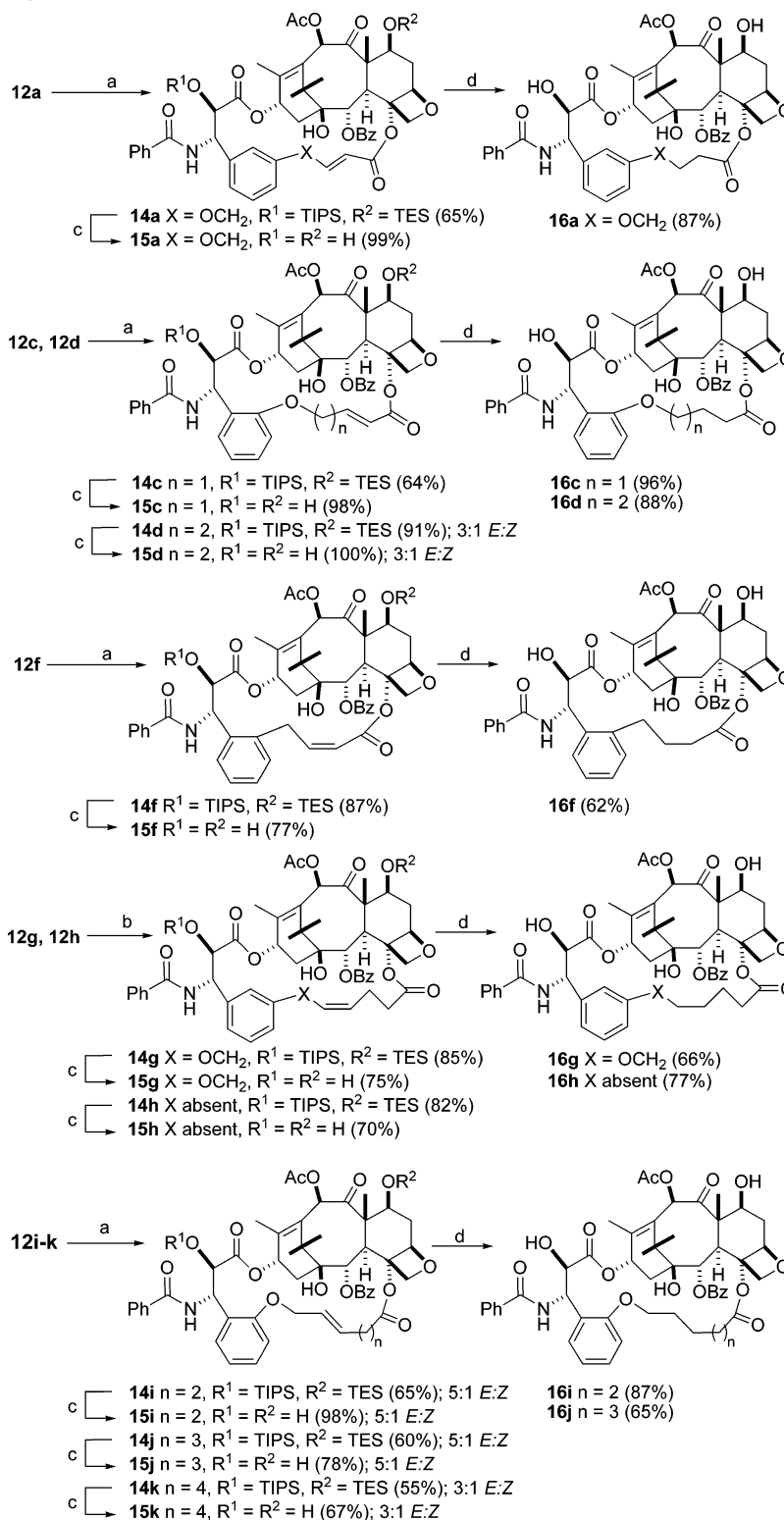
Molecular modeling studies of the interaction of macrocyclic taxoids linked from the ortho position of the C-3' phenyl group to the C-4 position indicated that these compounds are ideally suited to maintain the T-Taxol conformation while avoiding the unfavorable interaction with Phe270. Thus, these compounds were targeted as especially attractive candidates for synthesis. We adopted a similar ring-closing metathesis strategy to that used for **15g** and **15h** and subsequently synthesized the ortho-linked macrocyclic taxoids **15i–k** and their dihydro derivatives

16i,j with 8–10 atoms in the bridge, respectively. These compounds were approximately 10–130 fold less active than PTX in both cell lines. Interestingly, and in contrast to **15g** and **15h**, the open chain analogues **13i,j** were found to be inactive or only weakly active against the A2780 cancer cell line (Table 1).

At this point, we investigated the synthesis of compounds with shorter bridges. Thus, the two macrocyclic taxoids **15c** and **15d** and their saturated dihydro derivatives **16c** and **16d**, with six or seven atoms in the bridge between C-4 and the C-3' *o*-phenyl position of PTX were prepared. The compounds show approximately equal cytotoxicity to PTX against the A2780 ovarian cancer cell line but reduced activity against the PC3 prostate cancer cell line. Comprehensive conformational NMR/NAMFIS and docking studies indicated that compound **15c** was the best fit for the T-conformation of PTX. By modeling, this compound not only seats itself into the tubulin binding pocket, escaping the steric clash observed for meta-bridged compounds **15g** and **15h**,^{37,38} but it also nicely accommodates His227 of β -tubulin, allowing the imidazole ring to insert itself between the stacked rings (cf. Figure 2).³⁷

We sought to refine the bridge in **15c** further by shrinking the number of connecting atoms. Consequently the 17-membered macrocyclic taxoid **15f** and its saturated dihydro derivative **16f**, with 7 atoms in the bridge linking the ortho position of the C-3' phenyl to the C-4 position, were synthesized. Gratifyingly, the bridged taxoid **15f** exhibited excellent bioactivity. It is at least 50 times more potent than PTX against A2780, while its dihydro derivative **16f** shows about 30 times more activity than PTX against the same cell line. Both bridged taxoids also show slightly increased cytotoxicity compared with PTX against the PC3 cell line. The unusual activities of **15c,d**, **15f**, and **16c,d**, **16f** are not due to the substituents on the C-3' phenyl or the C-4 positions, since the open chain analogues **13c,d** and **13f** are almost completely inactive or weakly active against both the A2780 and PC3 cell lines (Table 1). This indicates that the activity associated with the bridged taxoids must originate from their conformational restriction.

Molecular modeling studies suggested that the *E* bridged macrocyclic analogue of **15f** should be more stable than *Z*-**15f**, while minireceptor QSAR⁵⁰ predicts this compound to be more active than PTX. On the basis of these projections, we investigated synthesis of the *E* macrocyclic bridged derivative of **15f**. Subjection of diene **12f** to ring-closing metathesis with Grubbs second generation catalyst in dichloromethane at an

Scheme 5. Synthesis of Bridged Paclitaxels **15** and **16**^a

^a a. (H₂IMes)(PCy₃)(Cl)₂Ru=CHPh, CH₂Cl₂, room temp; b. (PCy₃)₂(Cl)₂Ru=CHPh, DCM, room temp; c. HF, Py, THF, 0 °C to room temp d. H₂, Pd/C, 35 psi.

elevated temperature of 55 °C produced exclusively the isomerized product **17f**, which on deprotection with HF·Py furnished the isomerized *E* alkene **18f** (Scheme 6). This compound showed excellent cytotoxicity, almost equal to that of the *Z* bridged derivative **15f**, indicating that the precise stereochemistry of the bridging alkene linker causes only a small difference in the activity. The structure of **18f** was confirmed by hydrogenation to give a dihydro derivative identical with **16f**.

Synthesis of Bridged Paclitaxel Derivatives with Modified Pendent Groups. Having optimized the macrocyclic bridge between the C-4 acyl and the C-3' *o*-phenyl positions, we next investigated the structure–activity relationships at other sites of the bridged paclitaxel analogues in an attempt to identify additional paclitaxel analogues with further improved activity. We⁵¹ and others⁵² have previously reported the unusual cytotoxicity and *in vitro* tubulin polymerization activity of various

Table 1. Cytotoxicity and Tubulin Polymerization Activity of Macrocylic and Open Chain Paclitaxel Analogues

compound	IC ₅₀ values (nM) ^{a,b}		tubulin polym (ED ₅₀ , μM) ^{b,g}
	A2780	PC3	
PTX	15 ^c	5	0.5
13a	1900	550	1.0
13b	1700	320	1.0
13c	17800	2800 ^c	1.2 ^c
13d	19800	>13200	2.7 ^c
13e	1600 ^c	275	1.4
13f	1300 ^e	550	1.4
13g	770 ^c	128	0.42
13h	350	55	0.49
13i	2520	2600	1.8
13j	7400	4600 ^c	2.2
15a	6300	580	4.6 ^c
15c	14.5	15	0.28
15d	20 ^d	16	0.67
15f	0.3 ^d	2.5	0.3
15g	650	ND ^f	ND ^f
15h	680	34	1.6
15i	830	55	0.9
15j	440	90	0.53
15k	1840 ^c	500	0.93
16a	700 ^d	53	1.4
16c	18.5 ^d	50 ^c	0.83
16d	28	13	0.23
16f	0.5 ^d	2.4	0.21
16g	3600 ^c	1000	3.4 ^c
16h	8800	570	1.4
16i	980 ^c	51	0.76
16j	2000	390 ^c	0.85
18f	0.5 ^d	3.1	0.33
25	23.7 ^d	6	0.57 ^h
26	23.1 ^e	ND ^f	ND ^f
28	17.7 ^d	8.2	0.22 ^h
31a	1.4 ^d	3.2	0.49 ^h
31b	>6 ⁱ	11	0.35 ^h
32a	0.65 ^d	1.5	0.18 ^h
32b	0.49 ^d	1.3	0.22 ^h

^a Average of three determinations unless otherwise stated. ^b Standard error is less than 10% of the mean unless otherwise stated. ^c Standard error between 10% and 25% of the mean. ^d Standard error greater than 25% of the mean. ^e Single determination. ^f ND: Samples were not tested. ^g ED₅₀ values determined with GTP–tubulin unless otherwise stated. ^h ED₅₀ values for these samples were determined with GDP–tubulin and were normalized to the GTP–tubulin scale. ⁱ The value cited is the lower of two widely different determinations, probably due to solubility problems.

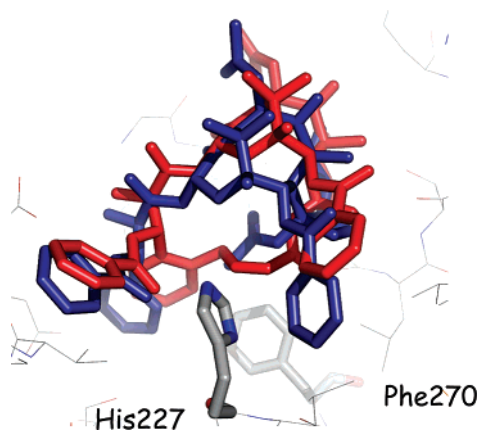


Figure 2. T-Conformations of PTX (blue) and **15f** (red) in the β -tubulin binding site, the latter having been docked by the Glide software. Both conformations were derived by NAMFIS analyses. His227 is shown in front of the structures, the **15f** bridge behind, and Phe270 (ref 49) further behind.

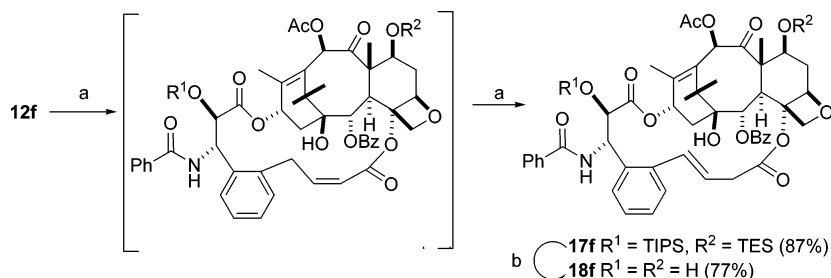
C-2 aroyl-substituted paclitaxel analogues, such as the C-2 *m*-methoxybenzoyl and *m*-azidobenzoyl derivatives. We thus embarked on the synthesis of the C-2 *m*-methoxybenzoyl

macrocylic paclitaxel analogue **28**. It was accomplished using modifications of known reactions. Thus 7,10,13-tris(triethylsilyl)-10-deacetylbaicatin (III) **19** was debenzoylated with Red-Al followed by protection as its cyclic carbonate **20**.²⁷ Compound **20** was treated with *m*-methoxyphenyllithium at 0 °C, followed by dimethylsilyl chloride to give **21** in 70% overall yield. Finally **21** was converted to the key intermediate **22** by steps similar to those of Scheme 2. Coupling of the building blocks **22** and **7g** under standard conditions⁴⁸ furnished the diene **23** in 70% yield. Ring-closing metathesis of diene **23** using second generation Grubbs's catalyst yielded the bridged taxoids **24** and **27** in a 3:1 ratio, with no formation of *E*-alkene. Interestingly, the first generation Grubbs's catalyst failed to bring about macrocyclization under various solvent and temperature conditions. The final compounds **25** and **28** were obtained by deprotection with HF·Py in tetrahydrofuran (Scheme 7), while hydrogenation of the two isomers delivered the same saturated compound **26**. Disappointingly, the macrocyclic bridged *m*-methoxy derivative **Z-28** and its isomer **25**, both showed reduced activity against the A2780 and PC3 cell lines compared with the corresponding C-2 benzoyl derivative **Z-15f**, and the dihydro derivative **26** was also less cytotoxic to the A2780 cell line (it was not tested against the PC3 cell line). The *N*-Boc derivatives **31a** and **32b** were however more promising, and in this series the C-2 *m*-methoxybenzoyl group did not reduce activity significantly in compounds **31a**, **32a**, and **32b**, in contrast to its effect on the *N*-benzoyl series. The reasons for this difference between the effects of the C-2 *m*-methoxybenzoyl group on the two different series are not clear. It is noteworthy that compounds **32a** and **32b** were the most potent compounds of the entire series against the PC3 cell line and also as promoters of tubulin polymerization.

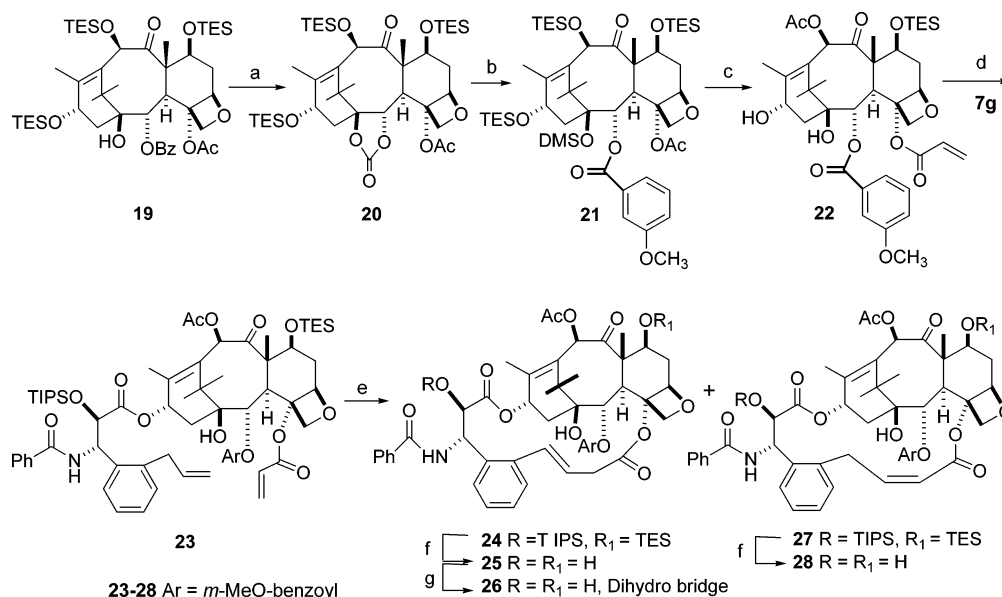
We then elected to carry out structural modifications on the side chain of the bridged paclitaxel analogues, since docetaxel with an *N*-Boc substituent has improved activity as compared with PTX. The β -lactam derivative **7h** was prepared by the procedure described Scheme 2. Coupling of **7h** individually with **11a** and **20** gave ω,ω' -dienes **29a** and **29b**, and these dienes upon ring-closing metathesis produced exclusively the cyclic double bond isomerized products **30a** and **30b**. None of the normal *Z* or *E* unisomerized alkenes were obtained in this reaction. The usual HF·Py deprotection produced the products **31a** and **31b**, and hydrogenation furnished the dihydro derivatives **32a** and **32b** (Scheme 8).

The bioactivities of compounds **31a**, **32a** and **32b** were 10–30-fold greater than those of PTX in the A2780 cell line, while in the PC3 cell line these compounds were 1.5 to 4-fold more potent than PTX, and **31b** was about half as potent as PTX in this cell line. Since the corresponding PTX analogues **15f** and **16f** are 30–50-fold more potent than PTX against the A2780 cell line and twice as potent as PTX against the PC3 cell line, it appears that the additional activities generally conferred by the *N*-Boc group and the *m*-methoxybenzoyl group are unique to the unbridged compounds. Modeling suggests a modest reorientation of the terminal phenyl rings in bridged compounds within the taxane binding site.⁵³ While the associated binding pose contributes to improved bridge-induced tubulin binding, it apparently dampens these additive substituent effects at the same time.

Historically, the search for microtubule modifiers has often been accompanied by a preliminary assessment of biological activity by examination of a drug's ability to polymerize tubulin or to influence the stability of microtubules. More recently, this practice has been largely supplanted by a focus on cytotoxicity.

Scheme 6. Synthesis of Bridged Paclitaxel **18**^a

^a a. Grubbs catalyst, CH_2Cl_2 , 55 °C, 77%; b. HF/Py, THF, 77%.

Scheme 7. Synthesis of Bridged Paclitaxels **25–28**^a

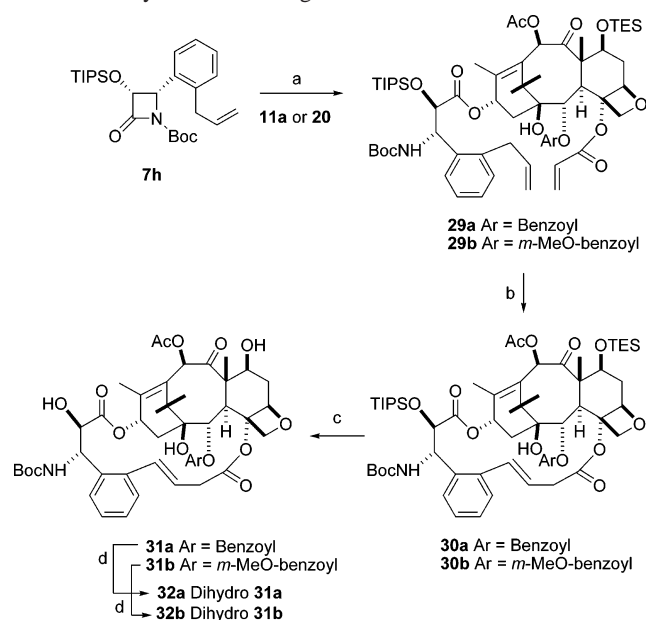
^a a. i, Red-Al, THF, 0 °C, ii, carbonyldiimidazole, imidazole, 33% (overall two steps); b. i, *m*-methoxyphenyl-MgBr, Et_2O , 0 °C, ii, DMSCl, imidazole, 70% (overall two steps); c. i, Red-Al, THF, 0 °C, 55%, ii, LHMDS, $\text{CH}_2=\text{CHCOCl}$, THF, 43%, iii, HF/Py, THF, 0 °C to room temp, 70%, iv, Ac_2O , CeCl_3 , THF, room temp, 90%, v, TESCl, imidazole, CH_2Cl_2 , 84%; d. LHMDS, THF, 90%; e. Grubbs catalyst (2nd), CH_2Cl_2 , room temp, 70%; f. HF/Py, THF, 80%; g. H_2 , Pd/C, MeOH, 60%.

The main reason, of course, is that an effective drug needs to penetrate the membrane of a cell to arrest microtubule function within its boundaries. Factors such as cell permeability, cytoplasmic metabolism, and nonselective binding are, of course, unexamined by an *in vitro* appraisal of the state of microtubule polymerization. As a consequence, in many cases where both polymerization and cytotoxicity data are available, a correlation fails to emerge. This is the case in the present study. For example, numerous analogues are equal to or within a factor of 2 relative to PTX in the polymerization assay, but 20–1200 fold poorer in the cell-based assays (e.g., **13a,b,c,g,h**, **15i,j**, and **16i,j**). By the same token, other *in vitro* analogues whose activities differ by a factor of 2 from PTX (**15c,d**, **25**, **28**, **31a**, **32b**) are nearly equivalent to PTX in their cellular action. Measurements of critical concentration and K_p , the equilibrium constant for polymer growth, would appear to be a much more reliable approach to assessment of biological activity.³⁷ Such measurements will be the subject of future work by our laboratories.

Resistance and the Bridged Analogues. An important discovery of the present work is that some of the bridged PTX analogues display promising activity against paclitaxel-resistant and epothilone A-resistant cell lines. The latter were derived by long-term exposure of 1A9 human ovarian carcinoma cells to PTX or epothilone-A (epo-A) in order to generate cells with drug-resistant clones. Subsequent molecular characterization of

these clones revealed that the resistance phenotype was due to distinct acquired β -tubulin mutations at the taxane binding pocket.^{54,55} As a result, PTX's ability to interact with the mutant tubulins in these clones is significantly impaired as evidenced by the lack of drug-induced microtubule-stabilizing activity and essentially lack of G2/M arrest.⁵⁶ Since drug resistance is the factor that hampers most PTX's clinical activity, we set out to test the activity of our analogues against the parental and drug-resistant cell lines (Table 2). While **13g** and **15c** exhibited similar or slightly improved activities over PTX, there are two compounds that stand out. Specifically the bridged taxoid **15f** and the dihydro analogue **16f** exhibit a remarkable activity in that not only are they about 100-fold more active than PTX against the parental 1A9 cells, but they are also 1200- and 150-times more effective than PTX (respectively) toward the PTX-resistant cell line PTX10 (Table 2). As shown by their relative resistance values, compound **15f** is able to completely overcome paclitaxel resistance (1.8 fold) as compared to 20-fold resistance exhibited by PTX. Compound **16f** is able to overcome paclitaxel resistance by 50%, while both compounds are 50 to 90 times more active than PTX against the epothilone-resistant 1A9-A8 cells. The relative potencies of these two compounds are unique.

The relative resistance values (RR) for 1A9-PTX10 cells across the compounds listed in Table 2 range from 2 to 21; those for 1A9-A8, from 3 to 82. The same quantities for **15f** and **16f** are perfectly normal by comparison, similar to PTX,

Scheme 8. Synthesis of Bridged Paclitaxels **31** and **32**^a

^a a. LHMDS, THF, 90%; b. Second generation Grubbs catalyst, CH₂Cl₂, RT, 70%; c. HF/Py, THF, 80%; d. H₂, Pd/C, MeOH, 60%.

Table 2. Bioactivity of Bridged Taxoids against Paclitaxel and Epothilone A Resistant Cell Lines^a

bridged taxanes	IC ₅₀ , nM ^b		RR ^c	IC ₅₀ , nM ^b		RR ^c
	1A9	1A9-PTX10 (Fβ270V)	PTX10/1A9	1A9-A8 (Tβ274I)	A8/1A9	
PTX	4.8 ± 4.5	157	20	21.5 ± 11.5	4.5	
13g	1.8 ± 2.5	65	18	148 ± 67.9	82	
13h	13.7 ± 8.6	42	5.5	137 ± 28.3	10	
15c	7.0 ± 0.85	126	17	26.5 ± 3.2	3.8	
15d	12.2 ± 7.0	157	9.2	46.4 ± 13.6	3.8	
15f	0.32 ± 0.35	0.13	1.8	0.27 ± 0.08	0.84	
15g	24.6 ± 9.0	196	6.3	> 300 ± 0.0	> 12	
15h	12.9 ± 7.5	157	21	> 300 ± 0.0	> 23	
16e	18.9 ± 1.27	35.9	1.8	66.5 ± 5.0	3.5	
16f	0.07 ± 0.02	1.03	12	0.44 ± 0.19	6.3	

^a 1A9 is the parental drug-sensitive cell line, 1A9-PTX10 is the paclitaxel resistant clone with an acquired Fβ270V (ref 49) mutation, and 1A9-A8 is the epothilone A resistant clone with an acquired Tβ274I mutation which also confers cross-resistance to paclitaxel (5–10 times). ^b The IC₅₀ values (nM) for each compound were determined in a 72-h growth inhibition assay using the sulforhodamine-B method as previously described (ref 55). All values represent the average of three or four independent experiments. ^c RR, relative resistance = IC₅₀ for resistant cell line/IC₅₀ for parental cell line.

and found in the windows RR = 0.8–2 and 6.8–12, respectively. The implication is that the bridged compounds, from the point of view of acquired resistance, are normal taxanes. The remarkable improvements of **15f** and **16f** over paclitaxel in apparently overcoming resistance owe their origin to an unusually high potency rather than to subtle structural features of the bridged molecules that enable them to bypass the mutated binding site residues.

Bridged Taxane Conformations in Solution. At the outset of our bridging studies, we hypothesized that creation of short bridges between the ortho-position of C-3' and the methyl of C-4 OAc as depicted in Figure 1 would lead to bioactive conformations in the T-Taxol family and provide highly active taxane analogues. Table 1 provides ample support for the concept and reinforces the proposition that deviations from ortho substitution and short tethers evoke a reduction in both cytotoxicity and tubulin polymerization. It would appear that

our initial conformational expectations have been fulfilled. However, we still lack an experimental structure of a bridged-taxane/tubulin complex and, thus, structural verification of the idea. We note that the two-carbon bridges between the C-3' and C-4 positions now enforce a 17-membered ring. While the latter involves two lactones, two C=C units, and seven bonds rigidified by the baccatin core, it is possible that the newly installed macrocyclic rings might sustain sufficient flexibility to require considerable conformational reorganization upon binding to tubulin. To examine this question, we performed empirical conformational analyses for two of our most active analogues, **15f** and **18f**. For both compounds, a quantitative NMR-ROESY determination was carried out. The corresponding cross-peaks were translated into intramolecular proton–proton separations based on internal distance standards. The corresponding distances were combined with taxane conformers derived by Monte Carlo conformational analyses within the NAMFIS framework.³⁵ As described in numerous previous studies, this technique is able to deconvolute an averaged NMR spectrum into a description of the ensemble of contributing conformations along with an estimate of the individual conformer populations.^{22,57}

As applied to **15f** with a cis double bond within the bridge, NAMFIS analysis, using 19 NMR-ROE-derived intramolecular atomic distances, delivered five conformations with estimated populations of 40, 27, 17, 9, and 7% (see Experimental Section). The top populated conformer is the T-form (40%), while the second and fourth most populated structures (27 and 9%, respectively) are slightly collapsed forms of the T-conformation in which the C3' benzamido phenyl to C2 phenyl centroid distance is 3 Å shorter. The third and fifth structures (17 and 7%, respectively) structures are somewhat extended structures that can be classified as neither T nor polar forms. Compound **18f** delivers a similar result, namely only three conformations from 15 ROE cross-peaks. One is the T-conformation (53%), the second, a slightly collapsed T-structure (33%), and the third, the polar conformer (14%). A similar analysis for parent PTX (**1a**) delivered T-conformers with much reduced populations of 2–5%.³⁷ Short-bridge ortho-tethering for this compound class increases the concentrations of the apparent bioactive conformers by 5–25 fold and thereby contributes to their exceptional activity. Figure 2 illustrates the superposition of PTX and **15f** in the β-tubulin binding cleft. The conformations of both molecules place the C-3' benzamido and C-2 benzoyl phenyls on either side of His227 (no π-stacking implied) and simultaneously avoid steric interaction with Phe270.⁴⁹

Conclusions and Perspectives

Over the past decade numerous bridging strategies have been explored in the effort to restrain the conformation of the paclitaxel architecture to its bioactive tubulin-bound conformation. Most have led to the synthesis of compounds that are considerably less potent than PTX.³³ A very few have demonstrated diminished cytotoxicity but matched the latter in a tubulin/microtubule *in vitro* assay.³² Our strategy was directed from the start by analysis of the T-Taxol conformation proposed as the binding geometry of PTX on β-tubulin.³⁶ Significantly, as depicted in Figure 1, it was predicted that a bridge between the methyl group of the C-4 acetate and the ortho-position of the C-3' phenyl group would lead to compounds that are constrained to adopt the bioactive molecular shape.

In the context of activity against A2780 ovarian cancer cells, the synthetic effort has led to seven compounds with activities equal to that of PTX (**15c,d**, **16c**, **25**, **26**, **28**, and **31a**), one that

is 3-fold more active (**32b**), three that are 30-fold enhanced (**16f**, **18f**, **31b**), and one that shows 50-fold improvement (**15f**). In the PC3 prostate cell line, the activity enhancements are somewhat less but are still significant (Table 1). Equally important, a subset of these compounds has been tested against both PTX- and epothilone-resistant cell lines (1A9-PTX10 and 1A9-A8, respectively, Table 2). Two of the most active compounds, **15f** and **16f**, are 1200- and 160-fold more active than PTX with respect to PTX10, respectively, and 90- and 50-fold more cytotoxic, respectively, against cells raised against epothilone-resistant cells (A8). Clearly, significant increases in antiproliferative activity can have a dramatic effect on resistance stemming from acquired mutations.

We have examined the origin of the bioactivities by seeking to define the degree of rigidification introduced by the C-4 to C-3' bridging principle. This has taken the form of extracting individual conformations associated with approximate populations from the averaged NMR spectrum of a compound. As applied to unconstrained PTX, the T-form was estimated to be present to the extent of 2–5% among eight diverse conformations.^{23,37} Constrained compounds **15f** and **18f**, on the other hand, appear in solution as five and three conformations, respectively, with 76% and 86% contributions from T-Taxol structures. While the significant activity increases measured for these substances cannot be attributed completely to conformational biasing, the results strongly suggest that this is a dominating factor.

If a given compound adopts the bioactive form, does this guarantee amplified activity? In a recent review of bridged taxanes we pointed out that enforcing the T-Taxol conformation is a necessary but not sufficient condition for eliciting high levels of drug potency.³³ In addition to the appropriate molecular conformation, the tubulin-taxane ligand must also adopt a compatible molecular volume. Compound **15g** with a 5-atom bridge between the meta position of the C-3' phenyl and the C-4 methyl carbon (*m*-O–CH₂–CH=CH–CH₂) illustrates the molecular dilemma. Like PTX it displays about 5% of the T-form in solution.³⁸ Unlike PTX, the compound is 4–45 fold less potent depending on cell line and 10-fold weaker as a tubulin polymerization agent. Modeling demonstrates that a section of the long, suboptimally substituted bridge falls outside the molecular volume of PTX and competes with tubulin's Phe270⁴⁹ for the same space within the binding pocket, as illustrated by Figure 3. Consequently, the ligand either rides higher in the pocket or is pushed out of it.³⁸ By contrast, compound **15c** (Table 1) with a three carbon ortho-bridge (*o*-O–CH₂–C=) likewise presents the T-form in solution, but the truncated bridge avoids a steric clash with the protein and results in activities equivalent to that of PTX.³⁷

Experimental Section

General Experimental Methods. All reagents and solvents received from commercial sources were used without further purification. ¹H and ¹³C NMR spectra were obtained in CDCl₃ on Varian Unity or Varian Inova spectrometers at 400 MHz or a JEOL Eclipse spectrometer at 500 MHz. High-resolution FAB mass spectra were obtained on a JEOL HX-110 instrument. Specific rotations were measured on a Perkin-Elmer 241 polarimeter. Usual workup was carried out by quenching the reaction, extracting the reaction mixture three times with EtOAc, combining the organic extracts, and washing the combined extracts with H₂O and brine, followed by drying over Na₂SO₄, filtration, and concentration of the organic solution to give crude product. MacroModel v7.2 and Maestro software were obtained from Schrödinger LLC (Portland, OR).

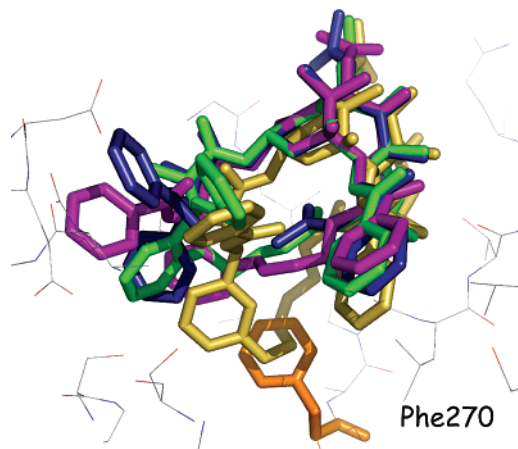


Figure 3. T-Conformation of PTX (blue) bound to β -tubulin. The T-conformers for the analogues *E*-**15c** (green), *Z*-**15g** (yellow), and *E*-**18f** (magenta) have been derived from NAMFIS analyses. The baccatin cores for PTX and the three analogues are superimposed. The meta-*Z*-bridged **15g** (yellow) is pushed out of the taxane binding site because phenylalanine 270 of tubulin (orange) is in steric conflict with the extended bridge, preventing effective binding to the protein. **15c** and **18f** avoid the Phe270 steric clash and fit nicely into the PTX binding site.

Representative Procedure for the Synthesis of β -Lactam Derivatives 7a–f. A typical procedure is described for the synthesis of these β -lactam derivatives.

(a) Synthesis of Racemic 1-(*p*-Methoxyphenyl)-3-acetyloxy-4-(*m*-allyloxyphenyl)azetidin-2-one (3a**).** To a solution of 3-(allyloxy)benzaldehyde (**1a**, 5 g, 34 mmol) in CH₂Cl₂ (85 mL) was added *p*-anisidine (4.38 g, 35 mmol), followed by MgSO₄ (50 g, in portions), and the resulting reaction mixture was stirred for 12 h. Removal of the MgSO₄ by filtration and concentration of the CH₂Cl₂ solution yielded crude imine **2a** (8.5 g). Diisopropylethylamine (100 mmol, 3 equiv) followed by acetoxyacetyl chloride (40 mmol, 1.2 equiv) were added to a solution of **2a** (8.5 g, 33 mmol) in CH₂Cl₂ (75 mL) at –78 °C, and the resulting solution was brought to room temperature over 12 h. The reaction mixture was concentrated, and the residue was purified by chromatography on silica gel using 10–20% EtOAc in hexane to furnish racemic 1-(*p*-methoxyphenyl)-3-acetyloxy-4-(*m*-allyloxyphenyl)azetidin-2-one (**3a**, 9.3 g, 75%).

(b) Resolution of **3a.** Lipase PS (Amano) (2 g) was added to a solution of **3a** (4 g, 10 mmol) in CH₃CN and pH 7 phosphate buffer (1:2.5), and the resulting solution was stirred at rt for 74 h. After usual workup the residue was separated by chromatography on silica gel to furnish (3*R*,4*S*)-1-methoxyphenyl-3-acetyloxy-4-(*m*-allyloxyphenyl)azetidin-2-one (**4a**) (1.92 g, 48%) and (3*S*,4*R*)-1-methoxyphenyl-3-hydroxy-4-(*m*-allyloxyphenyl)azetidin-2-one (1.84 g, 46%).

(c) Synthesis of (3*R*,4*S*)-1-Methoxyphenyl-3-triisopropylsilyloxy-4-(*m*-allyloxyphenyl)azetidin-2-one (5a**).** A solution of **4a** (920 mg, 2.5 mmol) in tetrahydrofuran (20 mL) was added dropwise to a stirred solution of 1 M KOH (1 M, 80 mL) and tetrahydrofuran (20 mL), and the resulting solution was stirred for 15 min. Addition of H₂O followed by usual workup produced (3*R*,4*S*)-1-methoxyphenyl-3-hydroxy-4-(*m*-allyloxyphenyl)azetidin-2-one (800 mg, 99%). To a solution of this alcohol (800 mg, 2.48 mmol) in *N,N*-dimethylformamide (3 mL) was added imidazole (500 mg, 7.4 mmol, 3 equiv) followed by Pr₃SiCl (508 mg, 2.65 mmol, 1.1 equiv), and the resulting solution was stirred at room temperature for 8 h. EtOAc was added to quench the reaction, and the usual workup followed by chromatography over silica gel with 2% EtOAc in hexane furnished (3*R*,4*S*)-1-methoxyphenyl-3-triisopropylsilyloxy-4-(*m*-allyloxyphenyl)azetidin-2-one (**5a**) (1.15 g, 99%).

(d) Synthesis of (3*R*,4*S*)-1-Benzoyl-3-triisopropylsilyloxy-4-(*m*-allyloxyphenyl)azetidin-2-one (7a**).** To a solution of **5a** (980 mg, 2.3 mmol) in CH₃CN (35 mL) was added ceric ammonium

nitrate (3.35 g, 6.1 mmol, 3 equiv) in H₂O (17 mL). The mixture was allowed to stand for 20 min at 0 °C and was then stirred for 45 min. EtOAc was added, and the organic phase was washed with saturated sodium metabisulfite. Usual workup followed by chromatography over silica gel with 10% EtOAc in hexane furnished the imide (3*R*,4*S*)-3-triisopropylsilyloxy-4-(*m*-allyloxyphenyl)azetid-2-one (**6a**, 600 mg, 78%). To a solution of **6a** (568 mg, 1.5 mmol) in CH₂Cl₂ (20 mL) were added triethylamine (0.63 mL, 4.5 mmol), dimethylaminopyridine (20 mg), and benzoyl chloride (0.52 mL, 4.5 mmol, 3 equiv) at 0 °C, and the resulting solution was stirred for 1 h. Usual workup followed by chromatography over silica gel with 2–5% EtOAc furnished (3*R*,4*S*)-1-benzoyl-3-*O*-triisopropylsilyloxy-4-(*m*-allyloxyphenyl)azetid-2-one **7a** (600 mg, 82%). **7a**: [α]_D²⁵ +97 (c = 0.4, CHCl₃). ¹H NMR (400 MHz) δ = 8.02 (2H, d, *J* = 7.3 Hz), 7.58 (1H, t, *J* = 7.3 Hz), 7.47 (2H, t, *J* = 7.4 Hz), 7.26 (1H, m), 6.98 (1H, d, *J* = 7.8 Hz), 6.94 (1H, dd, *J* = 1.9, 1.8 Hz), 6.86 (1H, dd, *J* = 7.3, 2.5 Hz), 6.02 (1H, m), 5.39 (1H, d, *J* = 6.1 Hz), 5.38 (1H, 2 × dd, *J* = 16, 6 Hz), 5.26 (1H, 2 × dd, *J* = 10.3, 1.6 Hz), 5.23 (1H, d, *J* = 6.1 Hz), 4.51 (2H, m), 1.00 (3H, m), 0.91 (4 s, 18H). ¹³C NMR (125 MHz) δ = 166.3, 165.4, 158.6, 135.4, 133.4, 133.3, 132.1, 129.9, 129.2, 128.2, 120.9, 117.6, 114.8, 114.7, 76.7, 68.9, 61.1, 17.5, 17.4, 11.7. HRFABMS: *m/z* calcd for C₂₈H₃₇NO₄Si⁺ 479.2492, found 479.2494 (Δ = 0.5 ppm). Characterization data for compounds **7b–d** and **7f,g** are provided in the Supporting Information.

Representative Procedure for the Synthesis of Baccatin III Derivatives 11a–d. Synthesis of 4-Deacetyl-4-acryloyl-7-*O*-triethylsilylbaccatin III (11a).

(a) **Synthesis of 1-Dimethylsilyl-4-deacetyl-4-acryloyl-4-deacetyl-7-*O*,10-*O*,13-*O*-tris-triethylsilylbaccatin III (9a).** Lithium hexamethyldisilazide (LiHMDS) (1 M, 1.3 mL, 1.3 mmol, 1.2 equiv) was added dropwise at 0 °C to a solution of 1-dimethylsilyl-4-deacetyl-7-*O*,10-*O*,13-*O*-tris-triethylsilylbaccatin III⁴⁶ (**8**) (1 g, 1.1 mmol) in THF (6 mL), and the resulting solution was stirred for 45 min. Acryloyl chloride (0.123 mL, 1.54 mmol, 1.3 equiv) was added to the above solution at 0 °C, and the reaction mixture stirred for 3 h. Saturated NH₄Cl solution (10 mL) was added, and the aqueous phase was subjected to the usual workup. The crude product as purified by chromatography over silica gel with 4% EtOAc in hexane to furnish 1-dimethylsilyl-4-deacetyl-4-acryloyl-7-*O*,10-*O*,13-*O*-tris-triethylsilylbaccatin III (**9a**) as a white solid (550 mg, 52%).

(b) **Synthesis of 4-Deacetyl-4-acryloyl-10-deacetyl-baccatin III.** To a solution of 1-dimethylsilyl-4-deacetyl-4-acryloyl-7-*O*,10-*O*,13-*O*-tris-triethylsilylbaccatin III (**9a**) (470 mg, 0.49 mmol) in THF (30 mL) was added dropwise HF•Py (70% HF, 2.37 mL) at 0 °C, and the resulting solution was brought to room temperature over 24 h, after which saturated NaHCO₃ solution (50 mL) was added carefully to quench the reaction. The aqueous phase was subjected to the usual workup, and the crude product was purified by preparative thin layer chromatography on silica gel developed with 70% EtOAc in hexane to give 4-deacetyl-4-acryloyl-10-deacetyl-baccatin III as a white solid (193 mg, 70%).

(c) **Synthesis of 4-Deacetyl-4-acryloylbaccatin III (10a).** Anhydrous CeCl₃ (20 mg) was added to a solution of 4-deacetyl-4-acryloyl-10-deacetyl-baccatin III (210 mg, 0.377 mmol) in THF (10 mL) and the resulting solution was stirred for 5 min. Acetic anhydride (0.65 mL, 14-fold excess) was added to the above solution and the reaction mixture was stirred for 4 h. EtOAc (100 mL) was added and the solution was washed with saturated NaHCO₃, water, and brine, dried over Na₂SO₄, and concentrated. The crude product was subjected to preparative thin layer chromatography on silica gel with 60% EtOAc in hexane to give 4-deacetyl-4-acryloyl-baccatin III (**10a**) as a white solid (200 mg, 96%).

(d) **Synthesis of 4-Deacetyl-4-acryloyl-7-*O*-triethylsilylbaccatin III (11a).** To a solution of 4-deacetyl-4-acryloylbaccatin III (**10a**) (50 mg, 0.083 mmol) in dichloromethane (5 mL) was added imidazole (56 mg, 0.836 mmol, 10 equiv) followed by triethylsilyl chloride (0.50 mmol, 6 equiv) at 0 °C, and the resulting solution was stirred for 3 h. Dilute HCl (0.05M, 5 mL) solution was added

to quench the reaction followed by EtOAc (40 mL). The organic phase was worked up in the usual way to give a crude product which was subjected to preparative thin layer chromatography over silica gel with 45% EtOAc in hexane to give **11a** as a white solid (40 mg, 72%). (**11a**): ¹H NMR (500 MHz, CDCl₃) δ = 8.11 (2H, d, *J* = 7.1 Hz), 7.59 (1H, t, *J* = 7.2 Hz), 7.46 (2H, t, *J* = 7.2 Hz), 6.52 (1H, dd, *J* = 17.4, 1.2 Hz, 1H), 6.47 (1H, s), 6.28 (1H, dd, *J* = 17.4, 10.5 Hz), 6.01 (1H, dd, *J* = 17.4, 1.2 Hz), 5.64 (1H, d, *J* = 6.8 Hz), 4.94 (1H, d, *J* = 7.7 Hz), 4.76 (1H, m), 4.53 (1H, dd, *J* = 10, 6.7 Hz), 4.33 (1H, d, *J* = 8.4 Hz), 4.20 (1H, d, *J* = 8.4 Hz), 3.94 (1H, d, *J* = 6.8 Hz), 2.55 (1H, m), 2.20 (3H, s), 2.22–2.10 (2H, m), 2.18 (3H, s), 1.90 (1H, m), 1.70 (3H, s), 1.18 (3H, s), 1.02 (3H, s), 0.91 (9H, t, *J* = 7.2 Hz), 0.60 (6H, m). ¹³C NMR (125 MHz) δ = 202.2, 169.4, 167.1, 165.3, 144.0, 133.7, 131.2, 130.1, 129.8, 129.6, 128.6, 84.2, 81.3, 78.8, 76.6, 75.8, 74.8, 72.4, 68.1, 58.8, 47.2, 42.8, 38.9, 37.3, 26.9, 21.0, 20.1, 14.9, 10.0, 6.84, 5.36. HRFABMS *m/z* calcd for C₃₈H₅₃O₁₁Si⁺ 713.3357, found 713.3326 (Δ = 4.4 ppm). Characterization data for compounds **11b–d** are provided in the Supporting Information.

Representative Procedures for the Coupling of Baccatin III Derivatives 11a–d with β-Lactam Derivatives 7a–d and 7f–g. A typical procedure is described for the synthesis of 3'-dephenyl-3'-(*m*-allyloxyphenyl)-4-deacetyl-4-acryloyl-7-*O*-triethylsilyl-2'-*O*-triisopropylsilylpaclitaxel (**12a**).

Synthesis of 3'-Dephenyl-3'-(*m*-allyloxyphenyl)-4-deacetyl-4-acryloyl-7-*O*-triethylsilyl-2'-*O*-triisopropylsilylpaclitaxel (12a). To a solution of baccatin III derivative **11a** (25 mg, 0.035 mmol) and β-lactam derivative **7a** (34 mg, 0.07 mmol, 2 equiv) in THF (6.5 mL) was added LiHMDS at –40 °C, and the resulting solution was stirred for 3 h. Saturated aqueous NH₄Cl (2 mL) was added to quench the reaction, and usual workup gave crude product which was purified by preparative TLC using 20% EtOAc in hexane as solvent to give **12a** (17 mg, 65%). ¹H NMR (400 MHz) δ = 8.10 (2H, dd, *J* = 7.2, 1.6 Hz), 8.00 (1H, m), 7.73 (2H, dd, *J* = 7.2, 1.6 Hz), 7.70–7.30 (8H, m), 7.04 (1H, d, *J* = 8.8 Hz), 6.98 (1H, d, *J* = 8 Hz), 6.90 (1H, bs), 6.85 (1H, d, *J* = 8 Hz), 6.63 (1H, d, *J* = 17.6 Hz), 6.52 (1H, d, *J* = 18.4 Hz), 6.47 (1H, s), 6.44 (1H, d, *J* = 10.4 Hz), 6.16 (1H, t, *J* = 7 Hz), 6.03 (2H, m), 5.93 (1H, d, *J* = 10.8 Hz), 5.72 (1H, d, *J* = 8 Hz), 5.59 (1H, d, *J* = 8.8 Hz), 5.42 (1H, dt, *J* = 17.2, 1 Hz), 5.29 (1H, dt, *J* = 10.4, 1 Hz), 4.90 (1H, d, *J* = 9.6 Hz), 4.87 (1H, s), 4.65 (2H, m), 4.33 (1H, d, *J* = 8.8 Hz), 4.26 (1H, d, *J* = 8.8 Hz), 3.90 (1H, d, *J* = 7.2 Hz), 2.58 (1H, m), 2.40 (1H, m), 2.17 (3H, s), 2.10 (1H, m), 2.08 (3H, s), 1.92 (1H, m), 1.74 (3H, s), 1.62 (3H, s), 1.22 (3H, s), 1.16 (3H, s), 0.95 (30H, m), 0.59 (6H, m). ¹³C NMR (100 MHz) δ = 202.0, 172.0, 169.5, 167.2, 167.0, 165.3, 159.2, 140.5, 140.4, 134.2, 133.7, 133.6, 133.3, 133.0, 131.9, 130.4, 130.1, 129.8, 129.6, 129.2, 128.9, 128.7, 127.7, 127.1, 118.9, 117.9, 114.5, 113.2, 84.4, 81.5, 79.0, 76.8, 75.3, 75.28, 75.22, 72.4, 71.7, 69.1, 58.6, 55.9, 47.0, 43.5, 37.4, 26.7, 21.8, 21.1, 18.0, 14.4, 12.7, 10.4, 6.9, 5.5. HRFABMS *m/z* calcd for C₆₆H₈₉NO₁₅Si₂Na⁺ 1214.5668, found 1214.5668 (Δ = 0 ppm). Characterization data for compounds **12b–f** are provided in the Supporting Information.

Representative Procedure for the Deprotection of 12a-i. Synthesis of 3'-Dephenyl-3'-(*m*-allyloxyphenyl)-4-deacetyl-4-acryloylpaclitaxel (13a).

To a solution of 3'-dephenyl-3'-(*m*-allyloxyphenyl)-4-deacetyl-4-acryloyl-7-*O*-triethylsilyl-2'-*O*-triisopropylsilylpaclitaxel (**12a**, 15 mg, 0.012 mmol) in THF (5 mL) was added hydrogen fluoride–pyridine complex (70%, 0.2 mL) at 0 °C, and the resulting solution was brought to room temperature overnight. Saturated NaHCO₃ solution (5 mL) was added carefully to quench the reaction. Usual workup followed by preparative TLC (silica gel, 50% EtOAc in hexane) furnished **13a** (5.5 mg, 55%). (**13a**): ¹H NMR (400 MHz, CDCl₃) δ = 8.15 (2H, d, *J* = 7.2 Hz), 7.72 (2H, d, *J* = 8 Hz), 7.61 (1H, t, *J* = 7 Hz), 7.50 (3H, m), 7.40 (3H, m), 7.10 (2H, m), 6.91 (1H, d, *J* = 7.6 Hz), 6.83 (1H, d, *J* = 9.2 Hz), 6.50 (1H, dd, *J* = 17.6, 1.2 Hz), 6.35 (1H, d, *J* = 10.4 Hz), 6.29 (1H, s), 6.1 (1H, m), 6.05 (1H, m), 5.68 (3H, m), 5.47 (1H, dd, *J* = 9.2, 1.6 Hz), 5.30 (1H, dq, *J* = 17.2, 1.6 Hz), 5.30 (1H, dq, *J* = 10.5, 1.2 Hz), 4.92 (1H, dd, *J* = 9.4, 1.6 Hz), 4.74 (1H, d, *J* = 2 Hz), 4.56 (2H, m), 4.48 (1H, dd, *J* = 10.4, 6.8 Hz),

4.34 (1H, d, $J = 8.4$ Hz), 4.25 (1H, d, $J = 8.4$ Hz), 3.86 (1H, d, $J = 6.8$ Hz), 2.58 (1H, m), 2.42 (1H, m), 2.30 (1H, m), 2.24 (3H, s), 1.90 (1H, m), 1.83 (3H, s), 1.70 (3H, s), 1.62 (1H, m), 1.22 (3H, s), 1.14 (3H, s). ^{13}C NMR (100 MHz) $\delta = 203.8, 173.3, 171.5, 167.2, 167.1, 165.4, 159.3, 142.3, 140.1, 133.9, 133.4, 133.2, 132.4, 132.1, 130.4, 130.2, 129.5, 129.3, 128.94, 128.91, 127.2, 119.6, 118.2, 114.5, 114.0, 84.6, 81.6, 79.1, 76.7, 75.8, 75.2, 72.7, 72.3, 72.2, 69.1, 58.8, 54.5, 45.9, 43.3, 35.9, 35.7, 32.1, 29.9, 27.0, 24.9, 22.9, 22.0, 21.0, 15.1, 9.8$. HRFABMS m/z calcd for $\text{C}_{51}\text{H}_{56}\text{NO}_{15}^+$ 922.3650, found 922.36676 ($\Delta = 2.9$ ppm). Similar procedures were employed to prepare compounds **13b–j**; characterization data for these compounds are provided in the Supporting Information.

Representative Procedure for Ring-Closing Metathesis of 12a–i. Synthesis of 7-O-Triethylsilyl-2'-O-triisopropylsilyl Bridged Paclitaxel 14a. Grubbs second generation catalyst (2 mg) in CH_2Cl_2 (2.5 mL) was added over 3 h to a solution of **12a** (16 mg, 0.013 mmol) in CH_2Cl_2 (4 mL), and the resulting solution was stirred for 1 h. The reaction mixture was concentrated, and the crude mass was applied to preparative thin layer chromatography using 25% EtOAc in hexane as solvent to furnish **14a** (10 mg, 65%). **14a:** ^1H NMR (500 MHz) $\delta = 8.10$ (2H, d, $J = 7.1$ Hz), 7.82 (2H, d, $J = 7.1$ Hz), 7.65 (1H, t, $J = 7.3$ Hz), 7.53 (2H, m), 7.45 (3H, m), 7.35 (1H, m), 7.21 (2H, m), 6.94 (2H, m), 6.46 (1H, s), 6.14 (1H, m), 6.12 (1H, d, $J = 16$ Hz), 5.73 (1H, d, $J = 7.3$ Hz), 5.5 (1H, d, $J = 6.6$ Hz), 4.93 (2H, m), 4.85 (1H, d, $J = 8$ Hz), 4.56 (1H, d, $J = 2$ Hz), 4.48 (1H, dd, $J = 10.5, 6.6$ Hz), 4.28 (2H, s), 3.81 (1H, d, $J = 7.1$ Hz), 2.50 (1H, m), 2.29 (1H, m), 2.18 (3H, s), 2.16 (1H, m), 2.08 (3H, s), 1.99 (3H, m), 1.91 (1H, m), 1.74 (3H, s), 1.24 (3H, s), 1.17 (3H, s), 1.10 (21H, m), 0.9 (9H, t, $J = 7.8$ Hz), 0.57 (6H, m). ^{13}C NMR (125 MHz) $\delta = 201.8, 171.5, 169.5, 167.3, 167.1, 164.1, 159.7, 147.0, 142.6, 140.5, 134.1, 134.0, 133.6, 132.0, 130.1, 130.0, 129.7, 128.9, 127.2, 123.8, 118.9, 118.2, 113.7, 84.4, 81.9, 79.1, 77.0, 75.2, 75.1, 72.7, 70.8, 70.0, 58.7, 57.6, 47.6, 43.4, 37.4, 35.9, 26.8, 21.6, 21.1, 18.1, 17.9, 14.5, 12.9, 10.3, 6.9, 5.5$. HRFABMS m/z calcd for $\text{C}_{64}\text{H}_{85}\text{NO}_{15}\text{Si}_2\text{Na}^+$ 1186.5355, found 1185.5330 ($\Delta = 2.2$ ppm). Similar procedures were employed to prepare compounds **14b–i**; characterization data for these compounds are provided in the Supporting Information.

Representative Procedure for the Deprotection of Macrocylic Paclitaxels 14a–j. Synthesis of Bridged Paclitaxel 15a. To a solution of **14a** (9 mg, 0.0077 mmol) in THF (3.5 mL) was added hydrogen fluoride–pyridine complex (70%, 0.15 mL) at 0 °C, and the resulting solution was brought to room temperature overnight. Saturated NaHCO_3 solution (5 mL) was added carefully to quench the reaction and after the usual workup resulted the crude product was purified by preparative TLC (silica gel, 60% EtOAc in hexane) to furnish **15a** (6.3 mg, 91%). **15a:** ^1H NMR (400 MHz) $\delta = 7.98$ (2H, d, $J = 7.6$ Hz), 7.80 (2H, d, $J = 7.6$ Hz), 7.69 (1H, t, $J = 7.6$ Hz), 7.61 (1H, t, $J = 6.8$ Hz), 7.53 (1H, m), 7.44 (2H, m), 7.22 (1H, dd, $J = 7.6$ Hz), 7.10 (1H, m), 7.05 (1H, bs), 6.98 (1H, m), 6.80 (1H, bs), 6.26 (s, 1H), 6.13 (1H, d, $J = 16$ Hz), 6.11 (1H, d, $J = 9.2$ Hz), 5.60 (1H, d, $J = 6.8$ Hz), 5.31 (1H, dd, $J = 9.3, 6.4$ Hz), 5.04 (1H, dd, $J = 14.4, 9.6$ Hz), 4.88 (2H, m), 4.48 (1H, d, $J = 9.6$ Hz), 4.37 (1H, m), 4.21 (2H, s), 3.68 (1H, d, $J = 6.8$ Hz), 2.58 (2H, m), 2.22 (3H, s), 1.90 (1H, m), 1.84 (3H, s), 1.78 (1H, m), 1.68 (3H, s), 1.53 (1H, m), 1.25–1.22 (1H, m), 1.21 (3H, s), 1.0 (3H, s). ^{13}C NMR (100 MHz) $\delta = 203.7, 173.0, 171.5, 169.3, 167.0, 163.6, 155.7, 143.3, 142.9, 138.4, 134.1, 133.6, 132.6, 132.4, 131.2, 130.1, 129.6, 128.9, 127.3, 126.8, 122.5, 119.3, 111.2, 84.3, 81.5, 79.4, 77.4, 76.7, 76.4, 75.7, 75.1, 72.5, 70.5, 66.1, 58.8, 58.6, 45.9, 43.2, 35.7, 35.0, 27.0, 22.3, 21.0, 14.8, 9.7$. HRFABMS m/z calcd for $\text{C}_{49}\text{H}_{52}\text{NO}_{15}$ 894.3337, found 894.3294 ($\Delta = 4.8$ ppm). Similar procedures were employed to prepare compounds **15b–j**; characterization data for these compounds are provided in the Supporting Information.

Representative Procedure for the Hydrogenation of Macrocylic Paclitaxels 15a–j. Synthesis of Dihydro Bridged Paclitaxel 16a. To a solution of **15a** (6 mg, 0.0067 mmol) in methanol (5 mL) was added 10% Pd–C (10 mg) and hydrogenated at 35 psi for 6 h. The reaction mixture was filtered a through short plug of silica gel, eluting with 20% methanol in EtOAc. The filtrate was

concentrated to crude mass, which was applied to silica gel preparative plate using 65% EtOAc in hexane as solvent provided the dihydro bridged paclitaxel **16a** (5 mg, 83% yield). **16a:** ^1H NMR (400 MHz) $\delta = 8.06$ (2H, d, $J = 7.2$ Hz), 7.82 (2H, d, $J = 7.2$ Hz), 7.10–7.03 (4H, m), 7.55–7.45 (4H, m), 7.19 (1H, t, $J = 7.6$ Hz), 7.08 (1H, bs), 6.96–6.88 (2H, m), 6.19 (1H, s), 6.14 (1H, t, $J = 8.8$ Hz), 5.57 (1H, d, $J = 7.2$ Hz), 5.24 (1H, dd, $J = 10.6, 6.8$ Hz), 4.89 (1H, d, $J = 8.4$ Hz), 4.62 (1H, m), 4.42 (2H, m), 4.32 (1H, m), 4.22 (1H, d, $J = 7.2$ Hz), 3.52 (1H, d, $J = 6.8$ Hz), 2.70 (1H, m), 2.50 (5H, m), 2.23 (1H, m), 2.22 (3H, s), 2.04 (3H, s), 1.88 (1H, m), 1.65 (3H, s), 1.60 (4H, m), 1.42 (3H, s), 1.10 (3H, s). ^{13}C NMR (100 MHz) $\delta = 203.6, 172.9, 171.5, 170.7, 167.0, 159.7, 142.7, 137.6, 134.2, 133.6, 133.5, 132.8, 132.4, 131.3, 130.4, 129.4, 129.07, 129.0, 127.4, 127.3, 122.1, 119.0, 109.6, 84.4, 80.9, 79.6, 76.3, 75.6, 74.9, 72.4, 70.5, 64.9, 64.5, 60.6, 59.7, 58.4, 45.7, 43.2, 38.3, 35.5, 35.1, 32.1, 31.4, 30.8, 29.92, 29.89, 29.5, 27.8, 27.1, 22.5, 21.0, 19.3, 14.7, 14.3, 13.9, 9.7$. HRFABMS m/z calcd for $\text{C}_{49}\text{H}_{54}\text{NO}_{15}\text{Na}^+$ 918.3313, found 918.3337 ($\Delta = 2.6$ ppm).

NAMFIS Analysis: 2D NMR-ROESY Spectra for 15f and 18f. The 1D ^1H assignments of **15f** and **18f** were accomplished by interpretation of the corresponding COSY, HMBC, and HSQC spectra. The 2D NMR ROESY analysis for both compounds was performed on an INOVA 400 MHz NMR spectrometer with 70, 100, 125, 150, 180 ms mixing times to check linearity of the cross-relaxation buildup rates. Interproton distances were calculated from the integrated cross-peak volumes using the initial rate approximation and an internal calibration distance between H-6a and H-6b of 1.77 Å. This provided 19 and 15 ROE-based interproton distances for **15f** and **18f**, respectively.

Solution Conformation Deconvolution for 15f and 18f. A 10 000-step conformational search was performed on both molecules with the MMFF94s force field and the GBSA/H₂O solvation model in MacroModel v7.2. An energy cutoff of 12 kcal/mol resulted in a pool of 93 and 374 unique conformations for **15f** and **18f**, respectively, with the global minimum found 62 and 29 times, respectively. The NAMFIS methodology integrated 19 ROE-determined distances measured in CDCl_3 and the 93 conformers of **15f** to deconvolute the NMR data into four conformations. One of these, however, places the C-4 acetate C=O beneath the oxetane ring. Inspection of literature X-ray structures of PTX and analogues shows that the carbonyl group consistently resides beneath the six-membered C-ring. Quantum chemical calculations (B3LYP/6-31G*, not shown) also demonstrate that oxetane orientation is ca. 4 kcal/mol higher in energy. Thus the 93 conformers were depleted of the latter conformation, and NAMFIS was rerun to give five conformations with populations of 40, 27, 17, 9, and 7%. (SSD = 59). The dominant conformer is the T-form (40%), while the second and fourth most populated structures (27 and 9%, respectively) are slightly collapsed variants of the T-conformation in which the C3'-benzamido phenyl to C2-phenyl centroid distance is 3 Å shorter. The third and fifth conformers (17 and 7%, respectively) are somewhat extended structures that can be classified as neither T nor polar forms. For **18f**, the 374 conformations likewise included a subset of carbonyl/oxetane structures, one of which appeared in the initial NAMFIS run employing 15 ROE-determined distances. These high-energy structures were removed from the dataset. A second NAMFIS run yielded three conformations with populations of 53, 33, and 14% (SSD = 96). One is the T-conformation (53%), the second, a slightly collapsed T-structure (33%), and the third, the polar conformer (14%).

Glide Docking. The top populated NAMFIS-derived conformation of **15f** was docked into the 1JFF tubulin pocket using Glide⁵⁸ in Maestro. An initial rigid dock of the ligand did not allow it to be situated in the pocket, so a follow-up flexible dock using the extra precision (XP) option was performed. It resulted in three very similar poses, all in the T-shape form, with the top pose differing from the NAMFIS conformation with an rms deviation of only 0.6 Å when all heavy atoms (C, N, O) were superposed.

Biological Data. IC₅₀ values were determined using the published method⁵⁹ for A2780 cells, the MTT assay⁶⁰ for PC3 cells, and the sulforhodamine-B method for the paclitaxel-resistant cell lines.⁵⁵

ED₅₀ values for induction of tubulin assembly were determined using either light scattering at 350 nm in a Hewlett-Packard 8453 absorption spectrometer or fluorescence in a 96-well plate format.⁶¹

Acknowledgment. This work was supported by the National Cancer Institute, National Institutes of Health (Grant CA-69571), and we are grateful for this support. We are likewise grateful to William Bebout and Rebecca Guza in the Department of Chemistry, Virginia Polytechnic Institute and State University, for mass spectra and preliminary cytotoxicity determinations, respectively. We are pleased to acknowledge the support and encouragement of Prof. Dennis Liotta (Department of Chemistry, Emory University).

Supporting Information Available: Characterization data for new compounds **7b–d,f,g**, **11b–d**, **12b–k**, **13b–j**, **14c,d,f–k**, **15c,d,f–k**, **16c,d,f–j**, **25**, **26**, **28**, **31a,b**, and **32a,b**; ¹H NMR spectra of compounds **15c,d,f**, **15f** (expanded), **15f** (COSY), **16c,f**, **25**, **31a,b**, and **32a,b**. This material is available free of charge via the Internet at <http://pubs.acs.org>.

References

- (a) Rowinsky, E. K.; The Development and Clinical Utility of the Taxane Class of Antimicrotubule Chemotherapy Agents. *Annu. Rev. Med.* **1997**, *48*, 353–374. (b) Crown, J.; O'Leary, M. The Taxanes: an Update. *The Lancet* **2000**, *355*, 1176–1178.
- Halkin, A.; Stone, G. W. Polymer-based Paclitaxel-eluting Stents in Percutaneous Coronary Intervention: A Review of the TAXUS Trials. *J. Intervent. Cardiol.* **2004**, *17*, 271–282.
- (a) Bollag, D. M.; McQueney, P. A.; Zhu, J.; Hensens, O.; Koupal, L.; Liesch, J.; Goetz, M.; Lazarides, E.; Woods, C. M. Epothilones, a New Class of Microtubule-stabilizing Agents with a Taxol-like Mechanism of Action. *Cancer Res.* **1995**, *55*, 2325–2333. (b) Kowalski, R. J.; Giannakakou, P.; Hamel, E. Activities of the Microtubule-stabilizing Agents Epothilones A and B with Purified Tubulin and in Cells Resistant to Paclitaxel (Taxol). *J. Biol. Chem.* **1997**, *272*, 2534–2541.
- ter Haar, E.; Kowalski, R. J.; Hamel, E.; Lin, C. M.; Longley, R. E.; Gunasekera, S. P.; Rosenkrantz, H. S.; Day, B. W. Discodermolide, a Cytotoxic Marine Agent that Stabilizes Microtubules More Potently than Taxol. *Biochemistry* **1996**, *35*, 243–250.
- Gapud, E. J.; Bai, R.; Ghosh, A. K.; Hamel, E., Laulimalide and Paclitaxel: A Comparison of their Effects on Tubulin Assembly and their Synergistic Action when Present Simultaneously. *Mol. Pharmacol.* **2004**, *66*, 113–121.
- Lindel, T.; Jensen, P. R.; Fenical, W.; Long, B. H.; Casazza, A. M.; Carboni, J.; Fairchild, C. R. Eleutherobin, a New Cytotoxin that Mimics Paclitaxel (Taxol) by Stabilizing Microtubules. *J. Am. Chem. Soc.* **1997**, *119*, 8744–8745.
- Schiff, P. B.; Fant, J.; Horwitz, S. B. Promotion of Microtubule Assembly in vitro by Taxol. *Nature* **1979**, *277*, 665–667.
- Horwitz, S. B. Mechanism of Action of Taxol. *Trends Pharmacol. Sci.* **1992**, *13*, 134–136.
- Jordan, M. A.; Toso, R. J.; Thrower, D.; Wilson, L. Mechanism of Mitotic Block and Inhibition of Cell Proliferation by Taxol at Low Concentrations. *Proc. Natl. Acad. Sci.* **1993**, *90*, 9552–9556.
- Blagosklonny, M. V.; Fojo, T. Molecular Effects of Paclitaxel: Myths and Reality (a Critical Review). *Int. J. Cancer* **1999**, *83*, 151–156.
- (a) Sunters, A.; Madureira, P. A.; Pomeranz, K. M.; Aubert, M.; Brosens, J. J.; Cook, S. J.; Burgering, B. M.; Coombes, R. C.; Lam, E. W. Paclitaxel-induced Nuclear Translocation of FOXO3a in Breast Cancer Cells is Mediated by c-Jun NH2-terminal Kinase and Akt. *Cancer Res.* **2006**, *66*, 212–220. (b) Faried, L. S.; Faried, A.; Kanuma, T.; Nakazato, T.; Tamura, T.; Kuwano, H.; Minegishi, T. Inhibition of the Mammalian Target of Rapamycin (mTOR) by Rapamycin Increases Chemosensitivity of CaSki Cells to Paclitaxel. *Eur. J. Cancer* **2006**, *42*, 934–947.
- Nogales, E.; Wolf, S. G.; Downing, K. H. Structure of the $\alpha\beta$ Tubulin Dimer by Electron Crystallography. *Nature* **1998**, *391*, 199–203.
- Lowe, J.; Li, H.; Downing, K. H.; Nogales, E. Refined Structure of $\alpha\beta$ -Tubulin at 3.5 Å Resolution. *J. Mol. Biol.* **2001**, *313*, 1045–1057.
- Dubois, J.; Guenard, D.; Gueritte-Voeglein, F.; Guedira, N.; Potier, P.; Gillet, B.; Betoel, J.-C. Conformation of Taxotere and Analogues Determined by NMR Spectroscopy and Molecular Modeling Studies. *Tetrahedron* **1993**, *49*, 6533–44.
- Williams, H. J.; Scott, A. I.; Dieden, R. A.; Swindell, C. S.; Chirlian, L. E.; Francl, M. M.; Heerding, J. M.; Krauss, N. E. NMR and Molecular Modeling Study of Active and Inactive Taxol Analogues in Aqueous and Non Aqueous Solution. *Can. J. Chem.* **1994**, *72*, 252–60.
- Cachau, R. E.; Gussio, R.; Beutler, J. A.; Chmurny, G. N.; Hilton, B. D.; Muschik, G. M.; Erickson, J. W. Solution Structure of Taxol Determined Using a Novel Feedback-scaling Procedure for NOE-restrained Molecular Dynamics. *Supercomput. Appl. High Perform. Comput.* **1994**, *8*, 24–34.
- Vander Velde, D. G.; Georg, G. I.; Grunewald, G. L.; Gunn, C. W.; Mitscher, L. A. "Hydrophobic Collapse" of Taxol and Taxotere Solution Conformations in Mixtures of Water and Organic Solvent. *J. Am. Chem. Soc.* **1993**, *115*, 11650–1.
- Paloma, L. G.; Guy, R. K.; Wrasidlo, W.; Nicolaou, K. C. Conformation of a Water-soluble Derivative of Taxol in Water by 2D-NMR Spectroscopy. *Chem. Biol.* **1994**, *1*, 107–12.
- Ojima, I.; Chakravarty, S.; Inoue, T.; Lin, S.; He, L.; Horwitz, S. B.; Kuduk, S. C.; Danishefsky, S. J. A Common Pharmacophore for Cytotoxic Natural Products that Stabilize Microtubules. *Proc. Natl. Acad. Sci. U.S.A.* **1999**, *96*, 4256–61.
- Ojima, I.; Kuduk, S. D.; Chakravarty, S.; Ourevitch, M.; Begue, J.-P. A Novel Approach to the Study of Solution Structures and Dynamic Behavior of Paclitaxel and Docetaxel Using Fluorine-Containing Analogues as Probes. *J. Am. Chem. Soc.* **1997**, *119*, 5519–27.
- Ojima, I.; Inoue, T.; Chakravarty, S. Enantiopure Fluorine-containing Taxoids: Potent Anticancer Agents and Versatile Probes for Biomedical Problems. *J. Fluorine Chem.* **1999**, *97*, 3–10.
- Snyder, J. P.; Nevins, N.; Cicero, D. O.; Jansen, J. The Conformations of Taxol in Chloroform. *J. Am. Chem. Soc.* **2000**, *122*, 724–5.
- Snyder, J. P.; Nevins, N.; Jimenez-Barbero, Cicero, D.; Jansen, J. M. Unpublished.
- Li, Y.; Poliks, B.; Cegelski, L.; Poliks, M.; Gryczynski, Z.; Piszczek, G.; Jagtap, P. G.; Studelska, D. R.; Kingston, D. G. I.; Schaefer, J.; Bane, S. Conformation of Microtubule-Bound Paclitaxel Determined by Fluorescence Spectroscopy and REDOR NMR. *Biochemistry* **2000**, *39*, 281–291.
- Barboni, L.; Lambertucci, C.; Appendino, G.; Vander Velde, D. G.; Himes, R. H.; Bombardelli, E.; Wang, M.; Snyder, J. P. Synthesis and NMR-Driven Conformational Analysis of Taxol Analogues Conformationally Constrained on the C13 Side Chain. *J. Med. Chem.* **2001**, *44*, 1576–1587.
- Boge, T. C.; Wu, Z.-J.; Himes, R. H.; Vander Velde, D. G.; Georg, G. I. Conformationally Restricted Paclitaxel Analogues: Macrocyclic Mimics of the "Hydrophobic Collapse" Conformation. *Bioorg. Med. Chem. Lett.* **1999**, *9*, 3047–52.
- Ojima, I.; Lin, S.; Inoue, T.; Miller, M. L.; Borella, C. P.; Geng, X.; Walsh, J. J. Macrocyclic Formation by Ring-closing Metathesis. Application to the Syntheses of Novel Macrocyclic Taxoids. *J. Am. Chem. Soc.* **2000**, *122*, 5343–53.
- Ojima, I.; Geng, X.; Lin, S.; Pera, P.; Bernacki, R. J. Design, Synthesis and Biological Activity of Novel C2–C3' N-Linked Macrocyclic Taxoids. *Bioorg. Med. Chem. Lett.* **2002**, *12*, 349–52.
- Geng, X.; Miller, M. L.; Lin, S.; Ojima, I. Synthesis of Novel C2–C3' N-Linked Macrocyclic Taxoids by Means of Highly Regioselective Heck Macrocyclization. *Org. Lett.* **2003**, *5*, 3733–6.
- Querolle, O.; Dubois, J.; Thoret, S.; Dupont, C.; Guéritte, F.; Guénard, D. Synthesis of Novel 2-O,3'-N-Linked Macrocyclic Taxoids with Variable Ring Size. *Eur. J. Org. Chem.* **2003**, 542–50.
- Querolle, O.; Dubois, J.; Thoret, S.; Roussi, F.; Montiel-Smith, S.; Guéritte, F.; Guénard, D. Synthesis of Novel Macrocyclic Docetaxel Analogues. Influence of Their Macrocyclic Ring Size on Tubulin Activity. *J. Med. Chem.* **2003**, *46*, 3623–30.
- (a) Querolle, O.; Dubois, J.; Thoret, S.; Roussi, F.; Guéritte, F.; Guénard, D. Synthesis of C2–C3' N-Linked Macrocyclic Taxoids. Novel Docetaxel Analogues with High Tubulin Activity. *J. Med. Chem.* **2004**, *47*, 5937–5944. (b) Geney, R.; Sun, L.; Pera, P.; Bernacki, R. J.; Xia, S.; Horwitz, S. B.; Simmerling, C. L.; Ojima, I. Use of the Tubulin Bound Paclitaxel Conformation for Structure-Based Rational Drug Design. *Chem. Biol.* **2005**, *12*, 339–348.
- Kingston, D. G. I.; Bane, S.; Snyder, J. P. The Taxol Pharmacophore and the T-Taxol Bridging Principle. *Cell Cycle* **2005**, *4*, 279–289.
- Guéritte-Voeglein, F.; Guénard, D.; Mangatal, L.; Potier, P.; Guilhem, J.; Césario, M.; Pascard, C. Structure of a Synthetic Taxol Precursor: N-tert-Butoxycarbonyl-10-deacetyl-N-debenzoyltaxol. *Acta Crystallogr. C* **1990**, *46*, 781–784.
- Cicero, D. O.; Barbato, G.; Bazzo, R.; NMR Analysis of Molecular Flexibility in Solution: A New Method for the Study of Complex Distributions of Rapidly Exchanging Conformations. Application to a 13-Residue Peptide with an 8-Residue Loop. *J. Am. Chem. Soc.* **1995**, *117*, 1027–33.

- (36) Snyder, J. P.; Nettles, J. H.; Cornett, B.; Downing, K. H.; Nogales, E. The Binding Conformation of Taxol in β -Tubulin: A Model Based on the Electron Crystallographic Density. *Proc. Natl. Acad. Sci. U.S.A.* **2001**, *98*, 5312–5316.
- (37) Ganesh, T.; Guza, R. C.; Bane, S.; Ravindra, R.; Shanker, N.; Lakdawala, A. S.; Snyder, J. P.; Kingston, D. G. I. The Bioactive Taxol Conformation on β -tubulin: Experimental Evidence from Highly Active Constrained Analogs. *Proc. Natl. Acad. Sci. U.S.A.* **2004**, *101*, 10006–10011.
- (38) Metaferia, B. B.; Hoch, J.; Glass, T. E.; Bane, S. L.; Chatterjee, S. K.; Snyder, J. P.; Lakdawala, A.; Cornett, B.; Kingston, D. G. I. Synthesis and Biological Evaluation of Novel Macrocyclic Paclitaxel Analogues. *Org. Lett.* **2001**, *3*, 2461–2464.
- (39) Paik, Y.; Yang, C.; Metaferia, B.; Tang, S.; Bane, S.; Ravindra, R.; Shanker, N.; Alcaraz, A. A.; Snyder, J. P.; Schaefer, J.; O'Connor, R. D.; Cegelski, L.; Kingston, D. G. I. REDOR NMR Distance Measurements for the Tubulin-Bound Paclitaxel Conformation. *J. Am. Chem. Soc.* **2007**, *129*, 361–370.
- (40) Tang, S.; Yang, C.; Brodie, P.; Bane, S.; Ravindra, R.; Sharma, S.; Jiang, Y.; Snyder, J. P.; Kingston, D. G. I. Bridging Converts a Noncytotoxic nor-Paclitaxel Derivative to a Cytotoxic Analogue by Constraining it to the T-Taxol Conformation. *Org. Lett.* **2006**, *8*, 3983–3986.
- (41) For the leading references, see: (a) Trnka, T. M.; Grubbs, R.H. The Development of $L_2X_2Ru=CHR$ Olefin Metathesis Catalysts: An Organometallic Success Story. *Acc. Chem. Res.* **2001**, *34*, 18–29, and references cited therein. (b) Fürstner, A. Olefin Metathesis and Beyond. *Angew. Chem., Int. Ed.* **2000**, *39*, 3012–3043. (c) Grubbs, R. H.; Chang, S. Recent Advances in Olefin Metathesis and its Applications in Organic Synthesis. *Tetrahedron* **1998**, *54*, 4413–4450, and references cited therein.
- (42) For the synthesis of various substituted racemic β -lactams, see: Carr, J. A.; Al-Azemi, T. F.; Long, T. E.; Shim, J.-Y.; Coates, C. M.; Turos, E.; Bisht, K. S. Lipase Catalyzed Resolution of 4-Aryl Substituted β -Lactams: Effect of Substitution on the 4-Aryl Ring. *Tetrahedron* **2003**, *59*, 9147–9160, and references cited therein.
- (43) Brievara, R.; Crich, J. Z.; Sih, C. J. Chemoenzymatic Synthesis of the C-13 Side Chain of Taxol: Optically Active 3-Hydroxy-4-phenyl β -lactam Derivatives. *J. Org. Chem.* **1993**, *58*, 1068–1075.
- (44) Substrates **4a–d** took 3–7 days for resolution using lipase PS, and substrate **4e** took 35 days for complete resolution.
- (45) For leading references, see: Littke, A. F.; Schwarz, L.; Fu, G. C. Pd/P(t-Bu)₃: A Mild and General Catalyst for Stille Reactions of Aryl Chlorides and Aryl Bromides. *J. Am. Chem. Soc.* **2002**, *124*, 6343–6348, and references cited therein.
- (46) Chen, S.-H.; Kadow, J. F.; Farina, V.; Fairchild, C. R.; Johnston, K. A. First Synthesis of Novel Paclitaxel (Taxol) Analogues Modified at the C4-Position. *J. Org. Chem.* **1994**, *59*, 6156–6158.
- (47) Holton, R. A.; Zhang, Z.; Clarke, P. A.; Nadizadeh, H.; Procter, D. J. Selective Protection of the C(7) and C(10) Hydroxyl Groups in 10-Deacetyl Baccatin III. *Tetrahedron Lett.* **1998**, *39*, 2883–2886.
- (48) (a) Holton, R. A.; Biediger, R. J.; Boatman, P. D. Semisynthesis of Taxol and Taxotere. In *Taxol: Science and Application*; Suffness, M., Ed.; CRC Press: New York, 1995; pp 97–121. (b) Georg, G. I.; Boge, T. C.; Cheruvallath, Z. S.; Clowers, J. S.; Harriman, G. C. B.; Hepperle, M.; Park, H. The Medicinal Chemistry of Taxol. In *Taxol: Science and Application*; Suffness, M., Ed.; CRC Press: New York, 1995; pp 317–375. (c) Ojima, I.; Habus, I.; Zhao, M.; Zucco, M.; Park, Y. H.; Sun, C. M.; Brigaud, T. New and Efficient Approaches to the Semisynthesis of Taxol and its C-13 Side Chain Analogs by Means of β -Lactam Synthon Method. *Tetrahedron* **1992**, *48*, 6985–7012. (d) Ojima, I.; Lin, S.; Chakravarty, S.; Fenoglio, I.; Park, Y. H.; Sun, C.-M.; Appendino, G.; Pera, P.; Veith, J. M.; Bernacki, R. J. Syntheses and Structure–Activity Relationships of Novel Nor-seco Taxoids. *J. Org. Chem.* **1998**, *63*, 1637–1645.
- (49) The reader should note that Phe272 is the pdb structure code for the Phe 270 sequence code (F β 270V) in Table 2.
- (50) Wang, M.; Xia, X.; Kim, Y.; Hwang, D.; Jansen, J. M.; Botta, M.; Liotta, D. C.; Snyder, J. P. A Unified and Quantitative Receptor Model for the Microtubule Binding of Paclitaxel and Epopthilone. *Org. Lett.* **1999**, *1*, 43–46.
- (51) Chaudhary, A. G.; Gharpure, M. M.; Rimoldi, J. M.; Chordia, M. D.; Gunatilaka, A. A. L.; Kingston, D. G. I.; Grover, S.; Lin, C. M.; Hamel, E. Unexpectedly Facile Hydrolysis of the 2-Benzoate Group of Taxol and Synthesis of Analogues With Improved Activities. *J. Am. Chem. Soc.* **1994**, *116*, 4097–4098.
- (52) (a) Ojima, I.; Kuduk, S. D.; Pera, P.; Veith, J. M.; Bernacki, R. J., Syntheses, and Structure–Activity, Relationships, of Nonaromatic, Taxoids: Effects, of Alkyl, and Alkenyl, Ester, Groups, on Cytotoxicity. *J. Med. Chem.* **1997**, *40*, 279–285. (b) Georg, G. I.; Harriman, G. C. B.; Ali, S. M.; Datta, A.; Hepperle, M.; Himes, R. H., Synthesis of 2-O-Heteroaryl Taxanes: Evaluation of Microtubule Assembly Promotion and Cytotoxicity. *Bioorg. Med. Chem. Lett.* **1995**, *5* (2), 115–118. (c) Nicolaou, K. C.; Renaud, J.; Nantermet, P. G.; Couladouros, E. A.; Guy, R. K.; Wrasidlo, W. Chemical Synthesis and Biological Evaluation of C-2 Taxoids. *J. Am. Chem. Soc.* **1995**, *117*, 2409–2420.
- (53) Alcaraz, A. A.; Mehta, A. K.; Snyder, J. P. The T-Taxol Conformation. *J. Med. Chem.* **2006**, *49*, 2478–2488.
- (54) Giannakakou, P.; Gussio, R.; Nogales, E.; Downing, K. H.; Zaharevitz, D.; Bollbuck, B.; Poy, G.; Sackett, D.; Nicolaou, K. C.; Fojo, T. A common pharmacophore for epothilone and taxanes: Molecular basis for drug resistance conferred by tubulin mutations in human cancer cells. *Proc. Natl. Acad. Sci. U.S.A.* **2000**, *97*, 2904–2909.
- (55) Giannakakou, P.; Sackett, D.; Kang, Y.-K.; Zhan, Z.; Buters, J. T. M.; Fojo, T.; Poruchynsky, M. S. Paclitaxel-resistant Human Ovarian Cancer Cells have Mutant β -Tubulins That Exhibit Impaired Paclitaxel-driven Polymerization. *J. Biol. Chem.* **1997**, *272*, 17118–17125.
- (56) Zhou, J.; O'Brate, A.; Zelnak, A.; Giannakakou, P. Survivin Deregulation in β -Tubulin Mutant Ovarian Cancer Cells Underlies Their Compromised Mitotic Response to Taxol. *Cancer Res.* **2004**, *64*, 8708–8714.
- (57) (a) Nevins, N.; Cicero, D.; Snyder, J. P. A Test of the Single-Conformation Hypothesis in the Analysis of NMR Data for Small Polar Molecules: A Force Field Comparison. *J. Org. Chem.* **1999**, *64*, 3979–3986. (b) Montegudo, E.; Cicero, D. O.; Cornett, B.; Myles, D. C.; Snyder, J. P. The Conformations of Discodermolide in DMSO. *J. Am. Chem. Soc.* **2001**, *123*, 6929–6930. (c) Thepchatri, P.; Cicero, D. O.; Montegudo, E.; Ghosh, A. K.; Cornett, B.; Snyder, J. P. Conformations of Laulimalide in DMSO-*d*₆. *J. Am. Chem. Soc.* **2005**, *127*, 12838–12846.
- (58) (a) Friesner, R. A.; Banks, J. L.; Murphy, R. B.; Halgren, T. A.; Klicic, J. J.; Mainz, D. T.; Repasky, M. P.; Knoll, E. H.; Shaw, D. E.; Shelley, M.; Perry, J. K.; Sander, L. C.; Shenkin, P. S. Glide: A New Approach for Rapid, Accurate Docking and Scoring. 1. Method and Assessment of Docking Accuracy. *J. Med. Chem.* **2004**, *47*, 1739–1749. (b) Halgren, T. A.; Murphy, R. B.; Friesner, R. A.; Beard, H. S.; Frye, L. L.; Pollard, W. T.; Banks, J. L. Glide: A New Approach for Rapid, Accurate Docking and Scoring. 2. Enrichment Factors in Database Screening. *J. Med. Chem.* **2004**, *47*, 1750–1759.
- (59) Louie, K. G.; Behrens, B. C.; Kinsella, T. J.; Hamilton, T. C.; Grotzinger, K. R.; McKoy, W. M.; Winker, M. A.; Ozols, R. F. Radiation Survival Parameters of Antineoplastic Drug-sensitive and Resistant Human Ovarian Cancer Cell Lines and Their Modification by Buthionine Sulfoximine. *Cancer Res.* **1985**, *45*, 2110–2115.
- (60) Chang, M. C.; Uang, B. J.; Wu, H. L.; Lee, J. J.; Hahn, L. J.; Jeng, J. H. Inducing The Cell Cycle Arrest and Apoptosis of Oral KB Carcinoma Cells by Hydroxychavicol: Roles of Glutathione and Reactive Oxygen Species. *Br. J. Pharmacol.* **2002**, *135*, 619–630.
- (61) (a) Chatterjee, S. K.; Barron, D. M.; Vos, S.; Bane, S. Baccatin III Induces Tubulin to Assemble into Long Microtubules. *Biochemistry* **2001**, *40*, 6964–6970. (b) Barron, D. M.; Chatterjee, S. K.; Ravindra, R.; Roof, R.; Baloglu, E.; Kingston, D. G. I.; Bane, S. A Fluorescence-Based High-Throughput Assay for Antimicrotubule Drugs. *Anal. Biochem.* **2003**, *315*, 49–56.